



Universidade Federal
do Rio de Janeiro
Escola Politécnica

ALMA: DIGITAL FLOWMETER FOR EMERGENCY MECHANICAL VENTILATOR SHARING DURING COVID-19 PANDEMIC

Mariana Tavares Pimenta

Projeto de Graduação apresentado ao Curso de Engenharia de Controle e Automação da Escola Politécnica, Universidade Federal do Rio de Janeiro, como parte dos requisitos necessários à obtenção do título de Engenheiro.

Orientadores: Claudio Miceli de Farias
Lilian Kawakami Carvalho

Rio de Janeiro
Junho de 2021

ALMA: DIGITAL FLOWMETER FOR EMERGENCY MECHANICAL
VENTILATOR SHARING DURING COVID-19 PANDEMIC

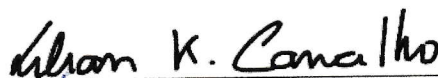
Mariana Tavares Pimenta

PROJETO DE GRADUAÇÃO SUBMETIDO AO CORPO DOCENTE DO
CURSO DE ENGENHARIA DE CONTROLE E AUTOMAÇÃO DA ESCOLA
POLITÉCNICA DA UNIVERSIDADE FEDERAL DO RIO DE JANEIRO COMO
PARTE DOS REQUISITOS NECESSÁRIOS PARA A OBTENÇÃO DO GRAU
DE ENGENHEIRO DE AUTOMAÇÃO.

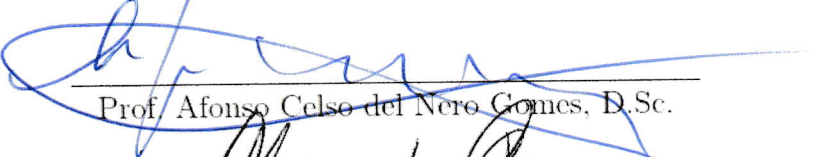
Examinado por:



Prof. Claudio Miceli de Farias, D.Sc.



Prof. Lilian Kawakami Carvalho, D.Sc.


~~Prof. Afonso Celso del Nero Comes, D.Sc.~~

Prof. Alexandre Visintainer Pino, D.Sc.

RIO DE JANEIRO, RJ – BRASIL
MARÇO DE 2021

Pimenta, Mariana Tavares

ALMA: Digital Flowmeter for Emergency Mechanical Ventilator Sharing During COVID-19 Pandemic/Mariana Tavares Pimenta. – Rio de Janeiro: UFRJ/ Escola Politécnica, 2021.

XIII, 59 p.: il.; 29, 7cm.

Orientadores: Claudio Miceli de Farias

Lilian Kawakami Carvalho

Projeto de Graduação – UFRJ/ Escola Politécnica/
Curso de Engenharia de Controle e Automação, 2021.

Referências Bibliográficas: p. 57 – 59.

1. Mechanical Ventilator.
2. Digital Flowmeter.
3. COVID-19. I. Farias, Claudio Miceli de *et al.* II. Universidade Federal do Rio de Janeiro, Escola Politécnica, Curso de Engenharia de Controle e Automação. III. Título.

*Aos meus pais,
Ary e Ana Paula,
e meus irmãos,
Luisa, Artur
e Gabriela.*

Agradecimentos

Agradeço a todos os muitos envolvidos na realização deste projeto, que tiveram enorme contribuição, durante um período de incertezas a respeito de uma doença desconhecida e perigosa, e que muitas vezes se expuseram, em prol da possibilidade de vir a ajudar a salvar vidas.

Ao Fabio Guimarães, pela participação desde o início do desenvolvimento prático do projeto, e pelo entusiasmo de alcançar resultados positivos.

Ao Alexandre Alexandria, pelas informações técnicas a respeito de peças e equipamentos médicos.

Ao Luis Filipe Kopp, por todas as peças cedidas durante a quarentena.

Agradeço imensamente aos pesquisadores do INMETRO, Jackson Oliveira, Carlos, Luciano Batista e Fábio Ouverney, que iluminaram o desenvolvimento do projeto com sua enorme experiência e conhecimento. Ao Fábio, agradeço também a oportunidade de dar continuidade a este desenvolvimento, no projeto que estamos realizando.

Agradeço ao Fernando Maia, ao Junior e ao Thierry da Brex Sistemas de Freios, pela usinagem das peças, durante as tentativas de fabricação do pneumotacômetro.

Ao professor Henrique Serdeira, agradeço pelo enorme apoio na montagem do projeto, e pelos ensinamentos recebidos.

Aos alunos do Labnet, em especial ao André, agradeço o apoio.

Agradeço à Luiza Nogueira, pelo projeto do pneumotacômetro em Autocad, e à Ágatha Pires por todas as simulações e auxílio na modelagem mecânica.

Ao Hospital da Polícia Militar de Niteroi, na figura da comandante Viviane Duarte e da cel. Eliana Vasconcelos, que disponibilizaram ventiladores mecânicos para a realização dos testes.

Agradeço aos meus orientadores, Lilian Kawakami e Claudio Miceli, que são para mim exemplos, e que me apoiaram além do âmbito acadêmico, e me incentivaram a descobrir novas capacidades com este projeto.

Agradeço aos professores Alexandre Pino e Afonso Celso, por aceitarem meu convite para participar desta banca. Ao professor Afonso Celso, agradeço com carinho também o apoio e atenção durante todos os anos da minha graduação.

Finalmente, agradeço especialmente à minha família, por todo o amor, felicidade

e suporte durante a minha formação pessoal e profissional. Em especial, ao meu pai, junto a quem a ideia deste projeto surgiu e cresceu.

Resumo do Projeto de Graduação apresentado à Escola Politécnica/ UFRJ como parte dos requisitos necessários para a obtenção do grau de Engenheiro de Automação.

**ALMA: FLUXÔMETRO DIGITAL PARA O COMPARTILHAMENTO
EMERGENCIAL DE VENTILADORES MECÂNICOS NO CONTEXTO DA
PANDEMIA DA COVID-19**

Mariana Tavares Pimenta

Junho/2021

Orientadores: Claudio Miceli de Farias
Lilian Kawakami Carvalho

Curso: Engenharia de Controle e Automação

Este projeto foi desenvolvido no contexto da pandemia da COVID-19, durante a qual diversos países relataram um número insuficiente de ventiladores mecânicos para tratamento dos pacientes. Medidas têm sido adotadas em estado de necessidade, incluindo o compartilhamento de um ventilador mecânico entre múltiplos pacientes. Um dos principais problemas desta estratégia é causado pelas complacências pulmonares distintas e variáveis dos pacientes, que resultam numa distribuição desigual de gás entre eles. Isso resulta na impossibilidade de controlar, ou mesmo medir, a vazão de ar entregue a cada paciente. O objetivo deste trabalho é o desenvolvimento de ALMA (**A**utonomous and **L**ow-cost **T**idal **V**olume **M**onitoring and **A**larming **d**evice), um fluxômetro digital, para possibilitar a supervisão do volume corrente entregue a cada paciente. O dispositivo desenvolvido é capaz de identificar se um paciente não estiver sendo adequadamente atendido por esta configuração, e alarmar a equipe médica responsável, aumentando a segurança dos pacientes durante o eventual compartilhamento de um ventilador.

Abstract of Undergraduate Project presented to POLI/UFRJ as a partial fulfillment of the requirements for the degree of Engineer.

ALMA: DIGITAL FLOWMETER FOR EMERGENCY MECHANICAL VENTILATOR SHARING DURING COVID-19 PANDEMIC

Mariana Tavares Pimenta

June/2021

Advisors: Claudio Miceli de Farias
Lilian Kawakami Carvalho

Course: Automation and Control Engineering

This project was developed in the context of the COVID-19 pandemic, during which the shortage of mechanical ventilators was pointed in several countries. Emergency measures included sharing a single mechanical ventilator between multiple patients. This approach is not recommended, due to the risks it introduces, but is used when strictly necessary. One of the main issues is the impossibility of controlling, or even measuring, the flowrate delivered to each patient. Different and changing lung compliances result in an unequal distribution of gas volume between patients, and may leave some of them insufficiently ventilated. The objective of this project is the development of ALMA (**A**utonomous and **L**ow-cost tidal volume **M**onitoring and **A**larming device), to enable supervision of the effectiveness of the tidal volume delivered to each patient. The device would identify whether a patient is not adequately attended to by this ventilation configuration and alarm the medical team in charge, thus increasing patient safety in the event of sharing a ventilator.

Contents

List of Figures	x
List of Tables	xiii
1 Introduction	1
1.1 Pandemic Context	1
1.2 Related Works on Sharing a Mechanical Ventilator	3
1.3 Proposal	5
1.4 Chapter Organization	5
2 Principles of Mechanical Ventilation	6
2.1 Respiratory Physiology	6
2.2 Mechanical Ventilation	11
2.3 Flowrate Measurement Systems in Medical Equipment	16
2.3.1 Variable Orifice Meter and its principle	17
2.3.2 Differential pressure transducer and specifications	18
3 ALMA - Autonomous and Low-cost tidal volume Monitoring and Alarming device	22
3.1 Overview and Components	23
3.2 Measuring System	24
3.3 Microcontroller Unit and Arduino IDE	28
3.4 Algorithm	29
4 Tests, Results and Discussion	34
4.1 Tests and Results	34
4.2 Discussion	43
5 Concluding Remarks and Future Work	46
5.1 Future Work	46
5.2 Conclusion	55
Bibliography	57

List of Figures

1.1	Ventilator sharing configuration [1]	2
2.1	Idealization of the Airways [2]	7
2.2	Cast of the Airways Without Alveoli [2]	7
2.3	Arrangement of the Pleural Sac - Top View [3]	8
2.4	Arrangement of the Pleural Sac - [4]	8
2.5	Contraction and Expansion of the Thoracic Cage [5]	9
2.6	Volume x Pressure curve of the Lung [2]	9
2.7	Average Lung Volumes and Capacities in a Young Adult Man [5]	10
2.8	Simplified Mechanical Model of the Respiratory System [6]	11
2.9	Phase Variables	13
2.10	Ventilation pressures	14
2.11	Target and Cycle Variables in Different Ventilator Settings [6]	14
2.12	Control Diagram of Ventilation	16
2.13	Variable Orifice Meter	17
2.14	Differential Pressure Sensor, Mp3v5010dp	17
2.15	Variable Orifice Meter under simulated flow.	18
2.16	Mp3v5010dp internal differential sensing element [7]	20
2.17	Mp3v5010dp response curve	20
2.18	Mp3v5010dp suggested decoupling circuit	21
3.1	ALMA Diagram. VOM - Variable Orifice Meter; DPS - Differential Pressure sensor; ADC - Analog to Digital Converter; HMI - Human Machine Interface.	24
3.2	Response curve experiment	25
3.3	Response Curve for VOM and DPS (Output voltage versus Reference flowrate).	25
3.4	Filtering and Decoupling Circuit with ADS1115	28
3.5	NodeMcu	29
3.6	NodeMcu - pinout	29

3.7	Flowrate derivative (dQ/dt) and inspiratory peak detection. The algorithm detects inspiration where the flowrate derivative surpasses a predetermined value. The flowrate (Q) is represented in blue, and its time derivative (dQ/dt), in orange.	31
3.8	Flowrate multiplied by its derivative ($Q \cdot dQ/dt$) and inspiratory peak detection. The algorithm detects inspiration where the defined variable for $Q \cdot dQ/dt$ surpasses a predetermined value. The flowrate (Q) is represented in blue, and $Q \cdot dQ/dt$, in grey.	32
4.1	Voltage output for various tidal volumes and linear behavior	35
4.2	Response curve after repeated calibration	35
4.3	Flowrate, $Q \cdot dQ/dt$ and integration beginning threshold (top); Flowrate, programmed tidal volume, and measured tidal volume (bottom), for a 600 ml/cycle tidal volume, under volume controlled ventilation	37
4.4	Flowrate, $Q \cdot dQ/dt$ and integration beginning threshold (top); Flowrate, programmed tidal volume, and measured tidal volume (bottom), for tidal volumes between 300 and 550 ml/cycle, under volume controlled ventilation. a) $V = 300 \text{ m}\ell$, b) $V = 350 \text{ m}\ell$, c) $V = 400 \text{ m}\ell$, d) $V = 450 \text{ m}\ell$, e) $V = 500 \text{ m}\ell$, f) $V = 550 \text{ m}\ell$	38
4.5	Reference volume and maximum measured volume, for each programmed tidal volume (top); Error bars in measured volumes (bottom)	39
4.6	Calculated volumes compared to ISO standards for Inspiratory Volume Monitoring [8], with reference tidal volume [$\text{m}\ell$] programmed on the ventilator represented on the x axis.	40
4.7	Flowrate, $Q \cdot dQ/dt$ and integration beginning threshold (top); Flowrate, minimum and maximum volumes displayed by the ventilator, and volumes measured by ALMA (bottom), for 15 cmH_2O peak inspiratory pressure, under pressure controlled ventilation	41
4.8	Flowrate, $Q \cdot dQ/dt$ and integration beginning threshold (top); Flowrate, minimum and maximum volumes displayed by the ventilator, and volumes measured by ALMA (bottom), for 12 to 30 cmH_2O peak inspiratory pressures, under pressure controlled ventilation. a) $P = 12 \text{ cmH}_2\text{O}$, b) $P = 18 \text{ cmH}_2\text{O}$, c) $P = 21 \text{ cmH}_2\text{O}$, d) $P = 24 \text{ cmH}_2\text{O}$, e) $P = 27 \text{ cmH}_2\text{O}$, f) $P = 30 \text{ cmH}_2\text{O}$	42
5.1	Machined FOM	47
5.2	Machined FOMs with smaller and larger orifice plates	47
5.3	Response curves for the original VOM (blue), the original FOM (orange) and the machined FOM with larger orifice plate (grey)	48

5.4	VOM mechanical model	48
5.5	VOM model displacement and stress simulations on ANSYS software	49
5.6	Calibration project schematics	51
5.7	ALMA and Ritter Flowmeters	52
5.8	Aalborg thermal mass flowmeter	52
5.9	Comparison between ALMA and Aalborg measurements	53
5.10	Comparison between ALMA and Aalborg measurements after Moving Average	53
5.11	Calibration results for the MUT after 6 rounds	54
5.12	Comparison between differential pressure measurements on the VOM with the Mp3v5010dp and FCO560 sensors	55

List of Tables

2.1 Ventilator Modes	15
3.1 Capacitance Values	27

Chapter 1

Introduction

1.1 Pandemic Context

Coronavirus disease (COVID-19) is an infectious disease caused by the newly discovered coronavirus, SARS-CoV-2. First cases were described in Wuhan, China, late December 2019, of what later developed into a pandemic. As of June, 2020, more than 10 million cases have been confirmed globally, and over 500 thousand deaths. Around 80% of patients recover from the disease without the need for hospitalization. The remaining 20% become seriously ill, with the highest risk being among the elderly and people with underlying medical conditions [9].

In its critical form, COVID-19 may cause respiratory failure and the patients' dependence on ventilatory support, which can prolong itself for several days [10, 11]. As the number of infected patients continues to rapidly rise, and critical symptoms suddenly manifest, a global surcharge of the healthcare system has settled in, with some of the biggest concerns being the availability of mechanical ventilators, and the duty of allocating patients for the available equipment.

The medical and scientific community has been aiming to provide alternative solutions to this shortage. While accelerating production of such equipment would be ideal, the market has been unable to meet the demand of ventilators and their building parts, however great the production and distribution efforts.

Several works have been made to allow for faster production of simpler, yet efficient ventilating equipment. However, the process of testing and validation, financing, production and distribution is often too long, and short term solutions are in order.

A risky suggestion, regarding the available equipment, seems to be sharing a single ventilator between multiple patients, i.e. connecting multiple sets of inspiratory and expiratory tubes in parallel to the same ventilator, as in the arrangement proposed by NEYMAN and IRVIN [12] (2006), exemplified in the diagram in Figure 1.1.

Although the non-standard use of the equipment is, as of yet, not recommended, and has been repeatedly debated in literature, such adaptation may become necessary as an emergency resource.

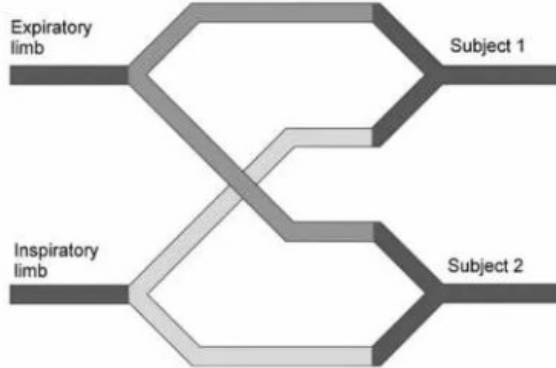


Figure 1.1: Ventilator sharing configuration [1]

The average adult mechanical ventilator is usually able to supply more than 2000 ml per cycle. The guidelines devised at the International Pulmonologist's Consensus on Covid-19 recommended ventilating patients at maximum pressure of 30 cmH₂O, with 4 to 6 ml/kg [10, 11], which is between 300 and 600 ml for most adult patients, for each ventilatory cycle. Therefore, the same ventilator could be able to meet the needs of up to four patients, as simulated by NEYMAN and IRVIN [12] (2006).

Previous research [12–14] (2006, 2008, 2012) has been made towards determining the safety of this adaptation. The most pressing problem of the shared system is caused by unequal characteristics of resistance and compliance of each patient and circuit. A patient's lung compliance is related to the organ's ability to expand and allow gas in. It is defined as the change in volume per unit change in pressure [2, 5]. These characteristics may be influenced by disease progression, previous health conditions or comorbidities of the patient, age, weight, reactions or movements, among others, and would result in a difficulty of dynamically controlling the gas flow to be received by each patient, as a more compliant lung would receive more volume than a less compliant one, under the same circumstances. This is even more important when observed that the patient's conditions will change in time, and most likely at different rates.

A mechanical ventilator can respond to system variations in real time, controlling the flowrate it sends to the patient. Yet, in a group of patients sharing the same device, the distribution of the total volume among more than one patient would prevent the ventilator from receiving feedback on variations of a specific one. This would endanger all patients, who might receive inadequate volume, either insufficient

or excessive. Delivering the correct amount of gases is imperative to avoid the increase in incidence of ventilator-induced lung injury [6, 15].

1.2 Related Works on Sharing a Mechanical Ventilator

NEYMAN and IRVIN [12] (2006) proposed and simulated the adaptation of a single ventilator for four patients and concluded that the volumes delivered by the equipment would be able to sustain up to four 70 kg patients. PALADINO *et al.* [13] (2008) extended the study by experimenting it with four adult sheep. However, stated that further studies would be necessary to conclude about patients with different lung compliances, and potential cross-contamination.

BRANSON and RUBINSON [16, 17] (2006, 2008) have repeatedly argued against the technique. The main concerns raised were the impossibility of detecting changes in an individual patient, and the alterations in tidal volume distribution caused by changes in compliance of each patient.

On another study, BRANSON *et al.* [14] (2012) simulated lungs of variable compliances and concluded that the tidal volume could not be controlled for each subject and the disparity was proportional to the variability in compliance.

CAVANILLES *et al.* [18] (1979) used a single ventilator with a modified circuit to individually ventilate the lungs of a patient. The system allowed control of tidal volume to each lung by altering resistance in the circuit, and included separate exhalation valves for different positive end-expiratory pressures. Separation of the exhaled gas would also limit the possibility of cross-infection.

More recent studies have also been trying to create safer arrangements. SOLIS-LEMUS *et al.* [19], RAREDON *et al.* [20] (2020, 2020) have simulated circuits with variable resistances and one-way valves to enable control of tidal volume delivered to each individual patient, for the case of different compliances.

A joint statement released by the Anesthesia Patient Safety Foundation (*APSF*) in March 2020 [21] strongly discourages this procedure, unless in grave temporary emergency, in absence of alternative reliable options. The list of concerns includes the unequal distribution of volume due to different lung compliances; impossibility to manage individual clinical improvement or deterioration, which may happen at different rates, even if clinical features are the same in the beginning of the treatment; difficulty or impossibility to individually monitor the patients' pulmonary mechanics and alarms, since the ventilator will only monitor the average pressures and volumes.

Additionally, *APSF* is concerned that this setting would make it impossible to manage positive end-expiratory pressure (*PEEP*) for each patient, which is an

important setting to avoid collapse of the alveoli. Individual PEEP managing may be possible with the addition of a pressure regulator or water column in each patient's expiratory circuit. In the case of different *PEEPs*, a one-way valve would also be necessary in every inspiratory line, to avoid backflow between patients.

Further dangers mentioned in the statement are the sensing of spontaneous breathing of a patient by the ventilator, which would affect the respiratory frequency of the group; and the failure of the ventilator's self-test, which is necessary to decrease measurement errors. In the event of a sudden deterioration of a single patient (e.g. a pneumothorax), the balance of ventilation would be distributed to the other patients. And in case of a cardiac arrest, ventilation to all patients would need to be stopped to allow the change to bag ventilation without aerosolizing the virus and exposing healthcare workers [21].

However, most patients in this critical state are maintained on sustained neuromuscular blockading agents, which would prevent spontaneous movements and breathing. Self-test could be performed before connecting other patients. For the shared setting, pressure-controlled ventilation could be recommended, under which no patient could receive a bigger volume than allowed by their lung compliance, although some might receive less volume than necessary in case of leakage. Finally, the same viral exposure risk occurs when disconnecting any infected patient from a ventilator, and it is possible to occlude the respective tube after removing the patient, normalizing the situation of the remaining patients. In every case, individual monitoring would be fundamental.

Another reason against the procedure is an ethical concern, of risking life-threatening treatment failure for all patients, when a ventilator might be able to save one of them individually. This scenario must therefore be discussed and agreed upon by the patients or their families, in case of absolute emergency.

The use of pulse oximetry has been considered as an option to aid with detection of hypoxemia, but the availability of oximeters for continuous use is also in question during a pandemic [17]. Also, it is slower in detecting inadequate ventilation, since oxygenated blood takes time to reach the limbs, and a new oxygen gradient will mask the actual values of gas exchange in the lungs before an equilibrium is reached.

As stated by the International Pulmonologist's Consensus on Covid-19 [10, 11], the high risk of running into shortage of ventilators during the pandemic may lead to the consideration of innovations such as connecting more than one patient to one ventilator. Although not recommended, such adaptation may become necessary.

1.3 Proposal

To address individual tidal volume monitoring problem, this project describes ALMA (Autonomous Low-cost Monitor and Alarm), a digital flowmeter, developed as an autonomous supervising device, independent of any parameters or information from the mechanical ventilation equipment. It dynamically analyses the gas flowrate in the tube and returns the tidal volume over the latest inspiratory cycle. Apart from performing volume integration, the device includes an alarm functionality that informs whether the patient connected to this line has not achieved a targeted tidal volume, which is easily set by the medical team.

The final device consists of a measuring system, a microcontroller, buttons and a display for efficient configuration and visualization, and a visual and sonorous alarm. When introduced in a patient's inspiratory line, it could allow minimal safety in emergency sharing of a mechanical ventilator between multiple patients. It may also be used solely as a flowmeter.

1.4 Chapter Organization

Chapter 2 presents a background for the development of the project, introducing basic concepts for understanding the respiratory system, mechanical ventilation and flowrate measurement. Chapter 3 introduces ALMA (**A**utonomous **L**ow-cost tidal volume **M**onitoring and **A**larming device), and explains its development process. Chapter 4 presents test results and a discussion of the device's utilization. Final considerations and future work will be discussed in chapter 5.

Chapter 2

Principles of Mechanical Ventilation

This chapter aims to present a theoretical background of the physiological and medical aspects of ventilation, and to discuss possibilities of flowrate measurement in medical devices. Concepts and definitions will be introduced, which were necessary for the development of the project. Section 2.1 will focus on the physiology of respiration. Section 2.2 will speak of mechanical ventilation and the main control modes used in respiratory medicine. Finally, section 2.3 will present flowrate measurement systems used in medical devices, and explain some choices made for this project.

2.1 Respiratory Physiology

The main function of the respiratory system is gas exchange: oxygen (O_2) is necessary for metabolic processes which liberate energy, while carbon dioxide (CO_2) one of the products of these processes, must be expelled. This section will focus on **pulmonary ventilation**, which stands for the inflow and outflow of air between the lungs and the atmosphere. It will also comment on how the anatomy of the airways facilitates diffusion of O_2 and CO_2 between the lung and the blood.

As represented by the drawing on figure 2.1, the airways consist of successively branching tubes, which become narrower, shorter, and more numerous, as we examine the lung deeper. The extremities of the tubes form small air sacs, the alveoli, which are wrapped by small blood vessels, the capillaries. The surface between the alveolar wall and the capillary wall is where the gas exchange between the blood and the air happens. Efficient diffusion of oxygen and carbon dioxide is enabled by two factors: the exceedingly thin barrier between blood and gas; and its large area, resultant of the several ramifications.

The first 16 generations of branches make up the conducting airways, whose function is to lead inspired air to the farther regions of the lung. They contain no alveoli and take no part in gas exchange, and have a volume of about 150 ml. The alveolated region of the lung where the gas exchange occurs is known as the

respiratory zone, and has a volume of about 2.5 to 3ℓ during rest (Figure 2.1). For visualization of the branching tubes, see figure 2.2, which shows a cast of the airways, without the alveoli.

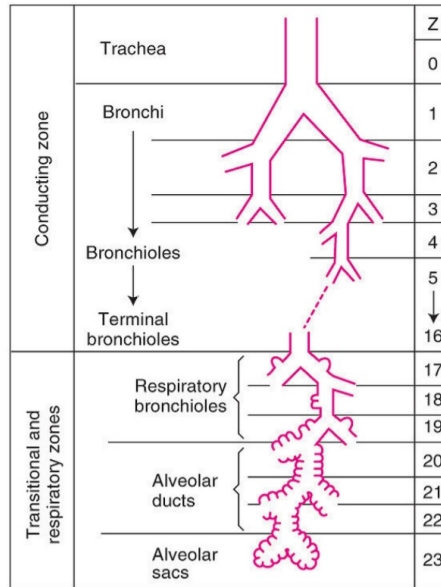


Figure 2.1: Idealization of the Airways [2]

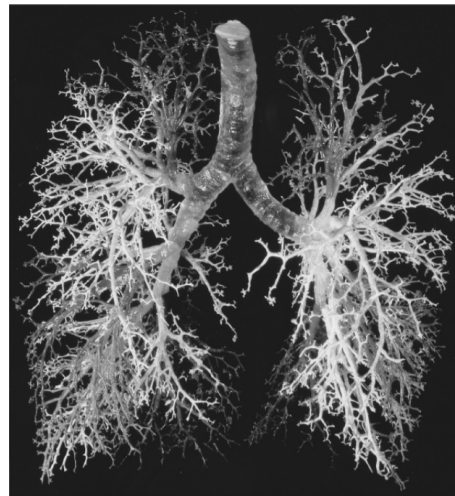


Figure 2.2: Cast of the Airways Without Alveoli [2]

The lungs are held to the chest wall by the pleura, an organ which is as a closed sac, with one of its walls attached to the lungs, and the other fixed to the internal side of the chest wall (Figures 2.3 and 2.4). There is little space inside the pleura, filled with liquid. This makes the pleural space almost indistensible, but well lubricated, allowing the lungs to freely slide as they expand and contract with the chest.

Normal pulmonary ventilation occurs with the expansion of the thoracic cavity, which in turn transmits to the expansion of the lungs. The increase of volume of

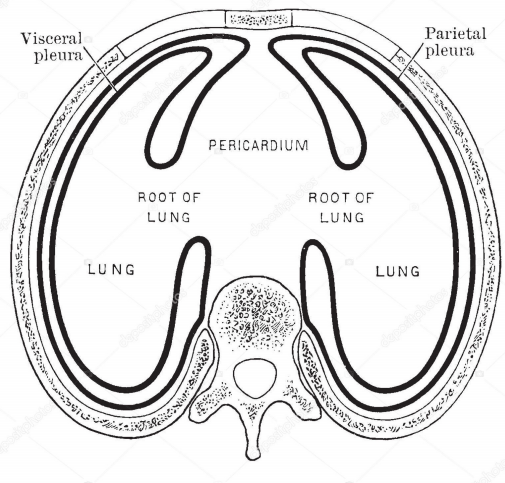


Figure 2.3: Arrangement of the Pleural Sac - Top View [3]

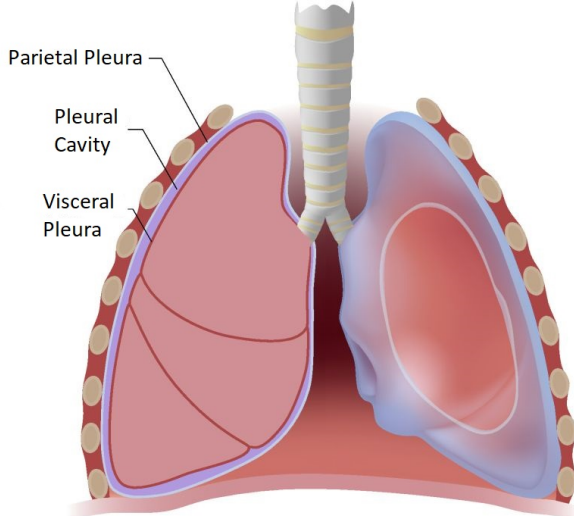


Figure 2.4: Arrangement of the Pleural Sac - [4]

the lungs, resultant of thoracic expansion, decreases their internal pressure, with respect to the atmosphere, drawing air in and resulting in inspiration.

The expansion of the thoracic cavity is mainly executed by the work of the *diaphragm* and the *external intercostal muscles*, thus spending energy. The most important muscle of inspiration is the *diaphragm*. When it contracts, the abdominal contents are forced downward and forward, and the vertical dimension of the chest cavity is increased. Contraction of the *external intercostal muscles* pull the ribs upward and forward, causing an increase in thorax diameter, horizontally.

Normal expiration is a passive motion, during rest. The elastic characteristics of the lung induce the return to the equilibrium position after being actively expanded during inspiration.

Figure 2.5 shows the muscular mechanics of pulmonary ventilation. To the left, the ribs during expiration are angled downward, and the external intercostals and di-

aphragm are relaxed. As they contract, the external intercostals pull the ribs forward and upward, and the diaphragm draws the lower surfaces of the lungs downward, thereby resulting in inspiration, on the right.

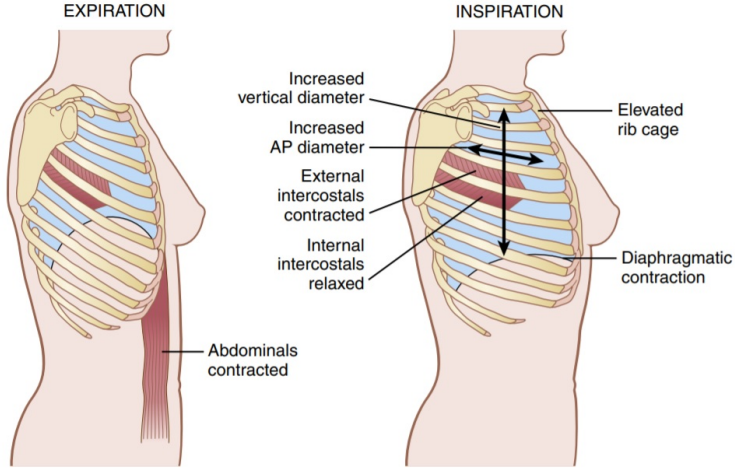


Figure 2.5: Contraction and Expansion of the Thoracic Cage [5]

"The extent to which the lungs expand for each unit increase in pressure (if enough time is allowed to reach equilibrium) is called **lung compliance**" [2]. Figure 2.6 shows the Volume x Pressure curve for a normal lung. Compliance is represented by the slope of the curve. In the normal range, the lung is very distensible or compliant. However, at high expanding pressures, it is stiffer, and its compliance is smaller. Notice there is some hysteresis between the inflation and deflation curves.

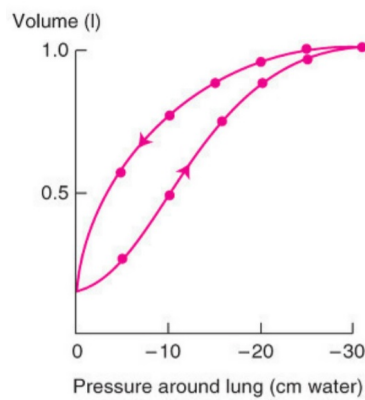


Figure 2.6: Volume x Pressure curve of the Lung [2]

Figure 2.7 shows the changes in lung volume during a series of breaths on a normal young adult man. Normal resting breathing can be seen as the regular cycles with an amplitude of about 500 ml, which is called tidal volume. The amplitude between a maximal inspiration and a maximal expiration is called vital capacity. Some gas remains in the lung after a maximal expiration, which is called residual

volume. The volume of gas in the lung after a normal expiration is the functional residual capacity.

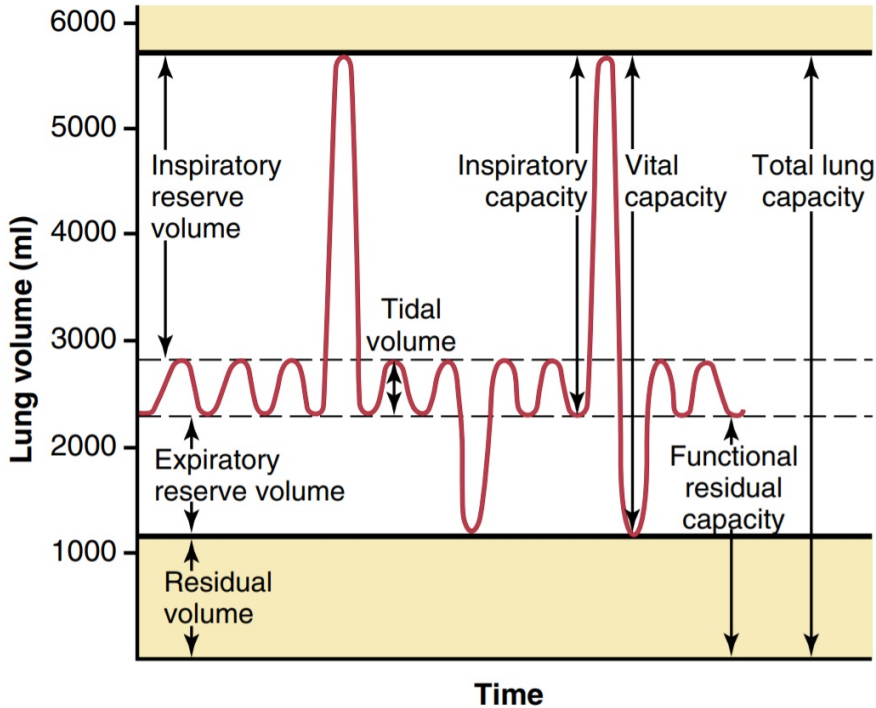


Figure 2.7: Average Lung Volumes and Capacities in a Young Adult Man [5]

Some important definitions follow:

Tidal Volume (V_t) is the volume of air inspired or expired with each normal breath; it is about 500 ml in the average healthy man.

Respiratory Rate (RR) is the number of breath cycles per unit of time (frequency). The normal rate is about 12 breaths/min.

Minute Respiratory Volume (\dot{V}) is the total amount of new air moved into the respiratory passages each minute, and is equal to the *tidal volume* times the *respiratory rate per minute*. The minute respiratory volume averages about $6 \text{ l}/\text{min}$.

$$\dot{V} = V_t \cdot RR \quad (2.1)$$

Lung tissue has elastic fibers, and a tendency to collapse. The thorax, on the other hand, if isolated, has a tendency to expand. United by the pleura, the equilibrium situation is such that the lung is distended, and the thorax, retracted, and no energy is expended. The volume occupying the lungs during rest is called functional residual capacity.

Inpiration is caused by a decrease of internal lung pressure, generated by thoracic expansion, with energy expenditure. Expiration happens passively in quiet breathing, and is mainly generated by the elastic properties of the lung. Lung collapse is avoided by pleural connection to the thorax.

2.2 Mechanical Ventilation

Contrary to natural respiration, which draws air into the lungs by expanding the thoracic cavity, and therefore decreasing internal pressure, mechanical ventilation usually accomplishes pulmonary ventilation by applying a positive pressure to the airways, resulting in inspiration.

Modeling

The respiratory system can be modeled as a flow resistance (consisting of the airways and tubes) connected to an elastic chamber (representing the lungs and chest wall), as seen on Figure 2.8 [6].

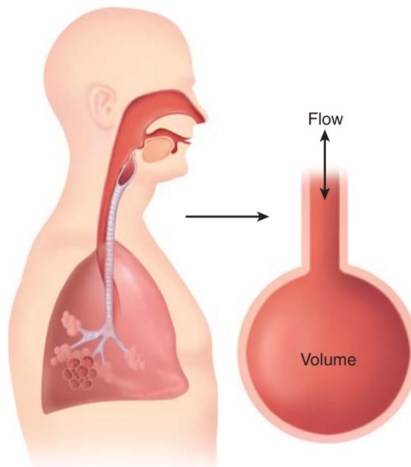


Figure 2.8: Simplified Mechanical Model of the Respiratory System [6]

The pressure required for a breath is determined by two components: i) an elastic component, due to the volume and elastic characteristics of the lungs; and ii) a resistive component, due to flowrate into the airways and the resistance of the tubes. The elastic behavior of the lungs is represented by their compliance, defined as the change in volume for a unit of pressure, i.e., $C(t) = \Delta V(t)/\Delta P(t)$. This ratio is variable, and inversely proportional to volume and pressure. The lungs are more compliant at smaller volume and pressure, and become stiffer as volume increases with pressure (see Figure 2.6, where the slope of the volume vs. pressure curve changes, and compliance is never constant). The second component, resistance, is the relationship between the pressure difference between the atmosphere and the lungs, and the flowrate ($Q = dV/dt$), i.e., $R = \Delta P/Q$.

Thus, the **Equation of Motion**, presented in Equation (2.2), describes inflation and deflation of the lungs. Compliance and resistance to flow are properties of the respiratory system. The pressure may be applied to the airways by a mechanical ventilator (P_{airway}), generated by the respiratory muscles (P_{mus}), or a combination

of both.

$$P_{airway} + P_{mus} = V/C(t) + R \cdot Q \quad (2.2)$$

where V is the volume, C is compliance, R is resistance to flow and Q is the instantaneous flowrate.

Control Variables

For a mechanical ventilator, any of these three variables (pressure, volume or flow) can be chosen as an independent variable (**control variable**), whose waveform can assume any predetermined shape during the ventilatory cycle (e.g. a step function). From the equation of motion, we observe that, since compliance and resistance are parameters of the patient, a ventilator can only control either pressure or volume or flowrate at one time. Because flowrate is the time derivative of volume, usual ventilator mode classifications consider either pressure or volume to be the control variables.

Phase Variables

Due to the periodicity of breathing, the ventilator must also be able to monitor and control a number of other variables that determine the phases of the respiratory cycle. The cycle is defined as the time span from the beginning of one breath to the beginning of the next. It may be divided into the following phases: the change from expiration to inspiration; inspiration; the change from inspiration to expiration; and expiration. A particular variable is measured and used to start, sustain, and end each phase. These are called **phase variables**, and can be specified as the trigger, limit, cycle and baseline variables [6] (see Figure 2.9) (3.10).

The **trigger variable** initiates inspiration. It is usually time, or a signal from the patient, indicating change in pressure or flowrate.

The **limit variable** is the pressure, volume, or flowrate that cannot be exceeded during the inspiratory phase. Inspiration is not necessarily terminated when the limit variable is reached, but it may mean the value must be sustained or even that the gas flow must stop until expiration.

The **cycle variable** can be pressure, volume, flow, or time, and is the condition for terminating inspiration.

Finally, a **baseline variable** is what is controlled during the expiratory.

The different types of phase variables can be analyzed in Figure 2.9. Notice the trigger variable causes inspiration to begin, while the cycle variable is responsible for the transition from the inspiratory to the expiratory phase. The rate of change

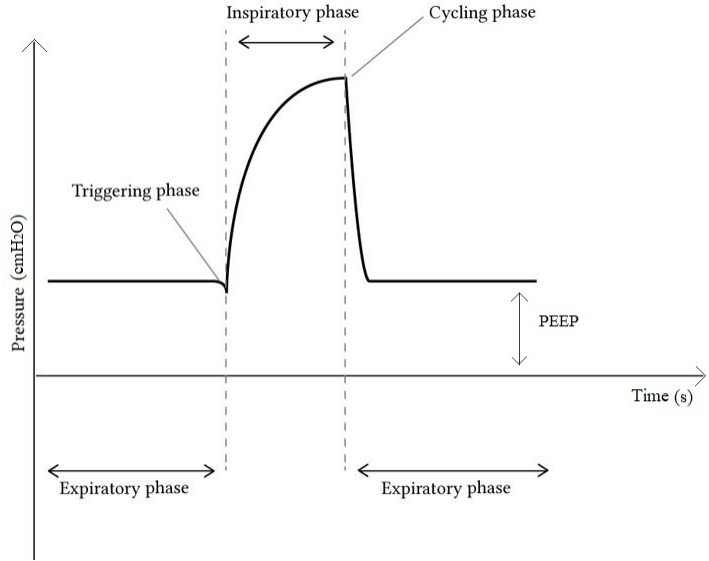


Figure 2.9: Phase Variables

of flowrate and pressure during inspiration depends on the control variable wave format.

Figure 2.10 presents a graph defining the most important pressures during mechanical ventilation. This is the case for volume control, and utilizing an inspiratory hold after achieving peak pressure. An inspiratory hold allows for the lungs to stabilize with the supplied volume, and the gas to evenly fill the available space. This will be used to explain the definitions of these terms, although not all of them are present in other ventilatory settings.

Positive Inspiratory Pressure or Peak Pressure (PIP) is the highest pressure achieved during inspiration. The **Plateau Pressure (P_{plat})** is the pressure after stabilization, during the **inspiratory hold**, when flow is paused, and volume is maintained inside the lungs. It is usual to maintain a positive pressure during expiration. This is necessary to avoid collapse of the lung alveoli, due to elasticity. It is called **Positive End Expiratory Pressure (PEEP)**, and is also the minimal pressure during the entire respiratory cycle. **PEEP** is one of the most important baseline variables.

Target x Cycle variables

To better explain target variables, we observe Figure 2.11, which illustrates pressure, volume and flowrate curves, for three different ventilator modes.

In **A**, inspiration is pressure-targeted and time-cycled. Notice pressure is set from the beginning of the cycle and maintained until the end of inspiration, which happens when the time limit is reached. Observe that in order to maintain pressure,

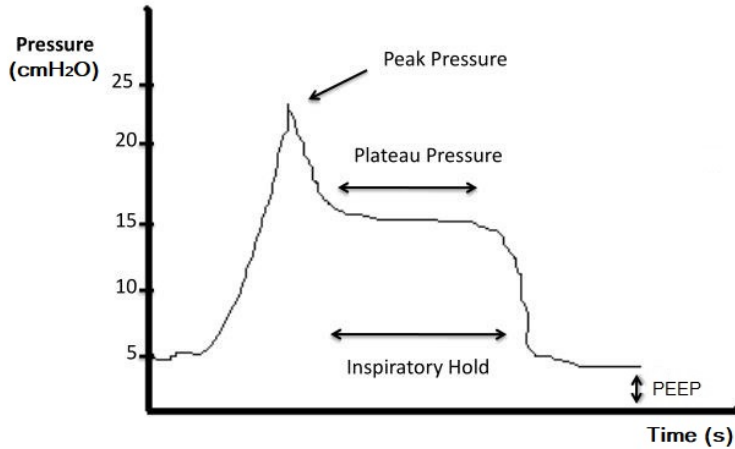


Figure 2.10: Ventilation pressures

flowrate must vary inversely to volume, as compliance naturally decreases with lung expansion, and is never constant.

B is an example of flowrate targeting. Volume is not targeted, but increases linearly, as it is the integral of flowrate. Volume is also working as the cycle variable. Expiration begins when the maximal volume is reached.

C targets both flowrate and volume, and it is visible that the targeted volume is maintained, once reached, while flow must then stop. Inspiration here is time-cycled. Pressure decreases slightly after flow is paused.

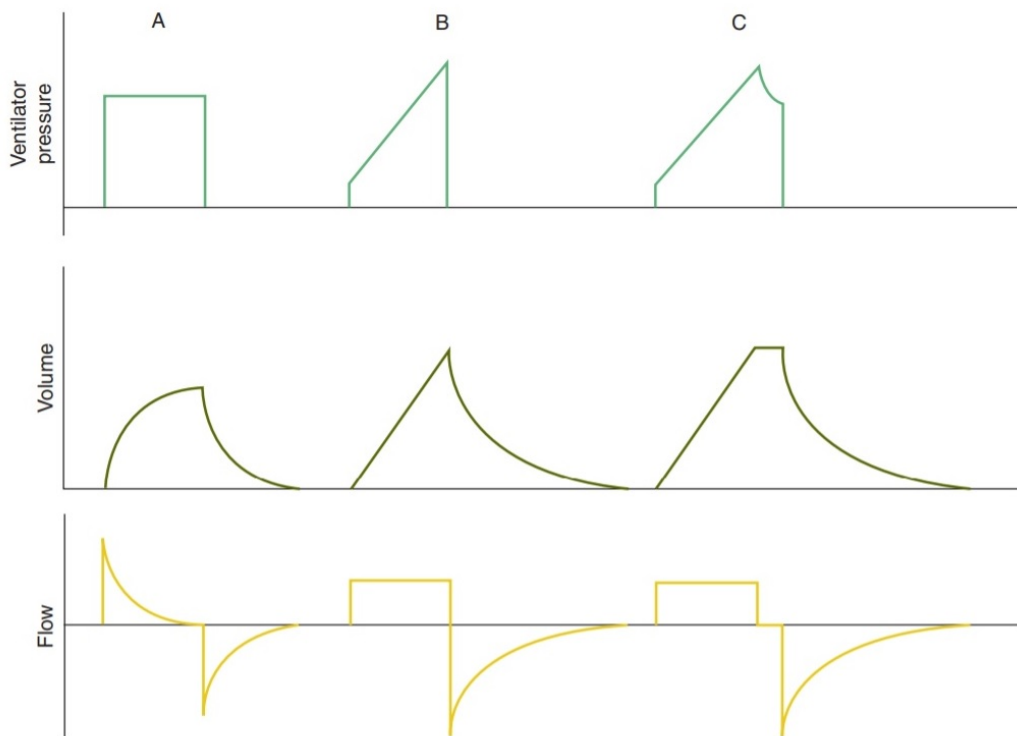


Figure 2.11: Target and Cycle Variables in Different Ventilator Settings [6]

Breath Sequences

It is possible, while artificially ventilating a patient, to provide two clinically different types of breaths: mandatory or spontaneous. Spontaneous breath is initiated and terminated by the patient. The patient's inspiratory effort may be assisted by the ventilator with a Continuous Positive Airway Pressure (*CPAP*) or with Pressure Support Ventilation (*PSV*). A mandatory breath, on the other hand, occurs when the ventilator determines either the beginning or the end of the breath. Three types of breath sequences may be generated from these approaches: **continuous mandatory ventilation - *CMV*** (all breaths are mandatory), **intermittent mandatory ventilation - *IMV*** (spontaneous breaths are permitted between mandatory breaths), and **continuous spontaneous ventilation - *CSV*** (all breaths are spontaneous).

Ventilation Modes

There are five basic ventilatory patterns, which may be characterized according to the following taxonomy: (a) Control Variable (volume-controlled or pressure-controlled), and (b) Breath Sequence (*CMV*, *IMV*, *CSV*). Additionally, modes may be distinguished by their trigger (start inspiration) and cycle (stop inspiration) variables. A summarizing table of the ventilation modes can be seen below, where *PC* stands for pressure-controlled, and *VC* for volume-controlled (Table 2.1).

Table 2.1: Ventilator Modes

Mode	Control variable; mandatory breath	Control variable; spontaneous breath	Name
CMV	volume pressure	none none	VC-CMV PC-CMV
CSV	none	pressure	CPAP or PSV
IMV	volume pressure	pressure pressure	VC-IMV PC-IMV

Control Diagram

The ventilator performs breath control in a feedback loop, where relevant variables are constantly monitored and used to determine the opening of the inspiratory and expiratory valves, therefore generating inspiration and expiration.

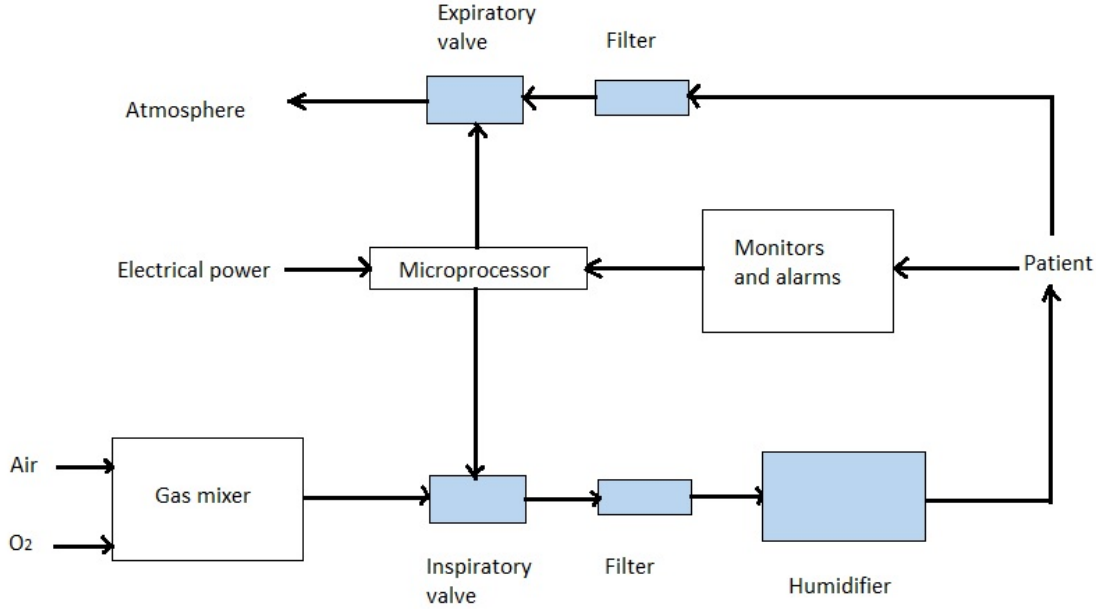


Figure 2.12: Control Diagram of Ventilation

COVID-19

The critical form of COVID-19 causes lung tissue inflammation, resulting in Acute Respiratory Distress Syndrome, or ARDS, which is characterized by increased work of breathing and oxygenation impairment. In such cases, "Respiratory support is indicated to reverse hypoxemia (below-normal level of oxygen in the blood) with the application of PEEP, delivery of a higher concentration of O_2 , and reduction of the work of breathing" [15].

2.3 Flowrate Measurement Systems in Medical Equipment

According to SCHENAA *et al.* [22], few kinds of flowmeters are used in the field of artificial ventilation for monitoring gas exchange. These must fulfill strict static and dynamic criteria, such as high sensitivity, good accuracy, low pneumatic resistance, short response time, adequate frequency response, among others. The most employed devices are fixed and variable orifice meters, hot wire anemometers, Fleisch pneumotachographs and ultrasonic flowmeters.

Orifice meters and Fleisch pneumotachographs require a secondary device (a differential pressure sensor) to perform the measurement of the resulting pressure differential between their upstream and downstream openings [22].

The chosen flowmeter for this project was a variable orifice meter (VOM) man-

ufactured by Vyaire Medical, shown in figure 2.13. The differential pressure sensor utilized was the Mp3v5010dp, from NXP, in figure 2.14. Their operating principles and properties will be described next.

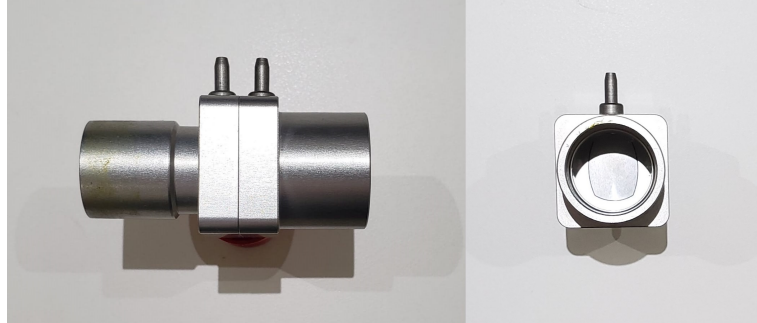


Figure 2.13: Variable Orifice Meter

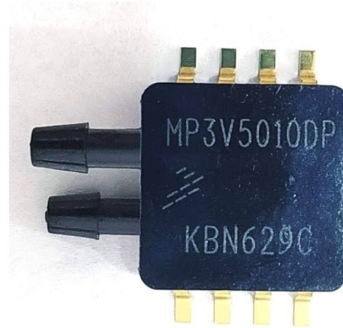


Figure 2.14: Differential Pressure Sensor, Mp3v5010dp

2.3.1 Variable Orifice Meter and its principle

The operating principle of orifice meters is to generate a pressure drop between the upstream and downstream sides of an orifice plate, which is placed in line with the pipeline where gas flow is running [14].

There are two types of orifice meters, with fixed or variable resistance. Fixed orifice meters (FOMs) present a square root relationship between the flowrate and the pressure drop, based on Bernoulli equation (2.3), where v is the fluid flow speed at a point on a streamline, g is the acceleration due to gravity, z is the elevation of the point above a reference plane, p is the pressure at the chosen point, and ρ is the density of the fluid at all points in the fluid.

$$\frac{v^2}{2} + gz + \frac{p}{\rho} = \text{constant} \quad (2.3)$$

The variable resistance is an advantage of variable orifice meters (VOMs) over FOMs, since it provides a linear response. As flowrate increases and becomes progressively turbulent, the hinged flap comprising these kinds of orifice plates opens,

mechanically lowering the resistance caused to the flow, and therefore resulting in a linear pressure drop, in response to gas flow (figure 2.15) SCHENAA *et al.* [22] (2015).

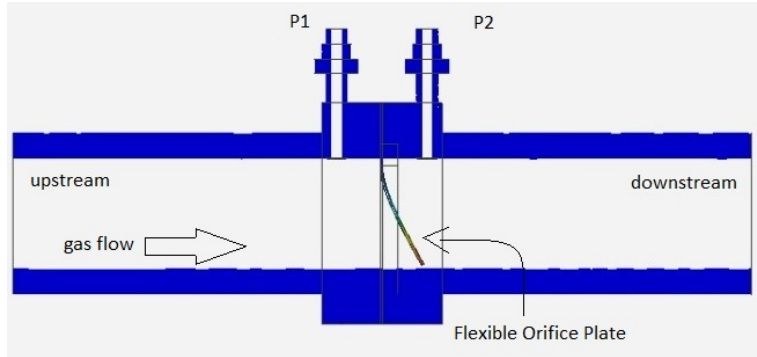


Figure 2.15: Variable Orifice Meter under simulated flow.

Further, this type of flowmeter is more robust and cheaper than hot wire anemometers, and does not suffer grave sensitivity changes due to condensation, as do Fleisch pneumotachographs [22].

It is important, in designing these types of orifice meters, to choose the appropriate elasticity and shape of the flap in the orifice, and many designs have been proposed and patented. The accuracy and the sensor response depend on the stress and strain characteristics of the variable orifice flap. This was the main difficulty found during the attempt made in reproducing these devices, discussed in section 5.1. A serial production of the flowmeters would resolve the bottleneck of manufacturing the final device, since the increased demand caused by the pandemic has made flowmeters almost unavailable in the market.

Due to the presence of a secondary sensing device to measure the pressure drop, the system's static characteristics such as accuracy, discrimination threshold (largest change in a value of a quantity being measured that causes no detectable change in the corresponding indication) and range of measurement, and dynamic characteristics, such as the time constant, are strongly influenced by the choice of an adequate differential pressure sensor [22], which will be discussed next.

Similar results may be obtained with the other kinds of meters. However, the VOM was the only one found available during the development of the project, and has shown good performance for the application.

2.3.2 Differential pressure transducer and specifications

A differential pressure sensor allows for a comparative measurement between two points, rather than an absolute measurement. The two pressures are applied to opposite sides of a single diaphragm. The deflection of the diaphragm, positive or

negative with respect to its resting state, determines the pressure difference. This way, measurements made are independent of atmospheric pressure. A scheme of this operation principle can be seen in Figure 2.16.

Because neither the pressure versus flowrate curve in the utilized VOM or the normal pressure drop in mechanical ventilation flowmeters were known, the choice of the DPS had to be made with little previous knowledge, and adapted throughout the project for its application. An initially available sensor was discarded after showing insufficient resolution to differentiate between the resulting pressures. However, these initial tests did not yet provide information on the VOM's pressure curve.

NXP's Mp3v5010dp was chosen next for the project, and is shown in Figure 2.14. Although the final pressure range of the VOM, which was discovered after calibration, was only approximately 6% of the Mp3v5010dp's response curve, the first measurements with the Mp3v5010dp showed a clear distinction of voltage outputs in relation to input flowrates to the VOM.

Another important characteristic of the Mp3v5010dp is that its zero value offset is around 0.300 V. The final calibration curve for the device in chapter 3 will show the range of voltage outputs for the application stood between 0.300 V and 0.500 V, with an angular coefficient of 0.0016 [V]/[L/min]. With such a large offset, the sensor choice could lead to measurement errors.

It is always advisable to work with a sensor with a range closer to the real inputs obtained in any application, and one which has a smaller zero offset. However, the higher price and difficulty of obtaining such a sensor in the market on a short timeline, especially during quarantine, discouraged the purchase of a better sensor. The goals of this project were to finish a working prototype as fast as possible, as well as to keep the final device within a possible budget, since this project was funded by personal funds.

The difficulties encountered due to the sensor choice required several other solutions and processing to be implemented, in order to reduce noise and error, and to increase precision of the final calculated volume, as will be further discussed in chapter 3. Better sensors could be used to perfect the device and further develop it.

Nevertheless, the final outcome of the project will prove to be acceptable for tidal volume measurement, according to the ISO standards used for comparison in chapter 4.

The Mp3v5010dp will be used to measure pressure drop in the VOM, which is directly related to flowrate in the tube. Its most important characteristics guaranteed by the maker are summarized below [7]:

- operational pressure range: 0 – 10 kPa (approximately 0 – 100 cmH_2O)
- supply voltage: 2, 7 – 3, 3 V

- sensor output: 0, 1 – 2, 7 V
- sensitivity: $27 \text{ mV/cmH}_2\text{O}$
- response time: 0, 1 ms

Figures 2.16 and 2.17 present the sensor's internal sensing element (the diaphragm), and response curve, respectively. For this specific DPS, $P_1 > P_2$, so the connection with the VOM's pressure outputs must obey the flow direction (P_1 is connected to the upstream output of the VOM, and P_2 , to the downstream output).

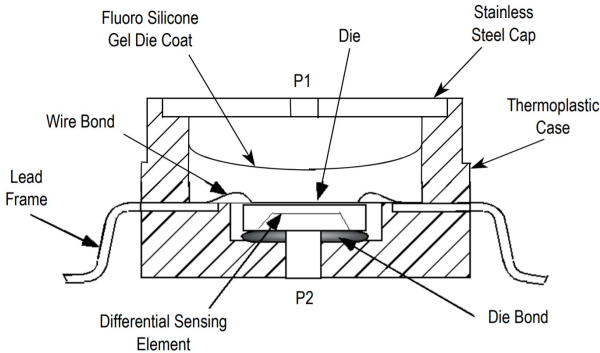


Figure 2.16: Mp3v5010dp internal differential sensing element [7]

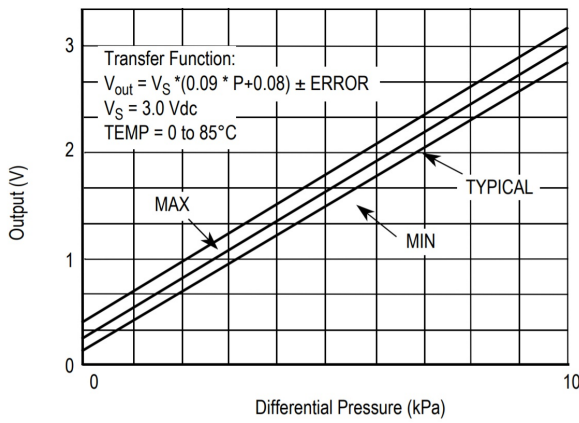


Figure 2.17: Mp3v5010dp response curve

As previously stated, the differential pressure sensor is crucial in determining the final characteristics of the measuring system, such as accuracy, discrimination threshold, range of measurement, dynamic response. The calibration curve and studied characteristics of the measurement system, considering the VOM connected to the DPS will be presented in section 3.2. For the scope of the project, however, dynamic characteristics were not studied, and must be further analysed in future works.

Finally, figure 2.18 presents the maker's suggested decoupling circuit. For this project, the $1 \mu F$ capacitor will be used as a decoupling capacitor.

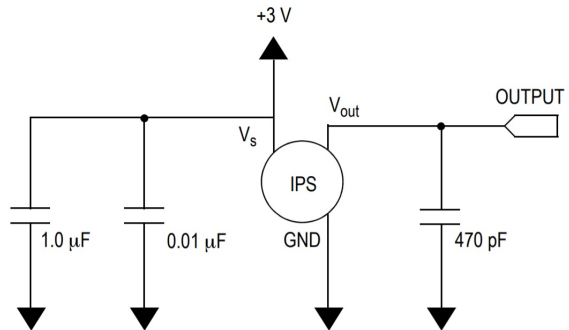


Figure 2.18: Mp3v5010dp suggested decoupling circuit

Chapter 3

ALMA - Autonomous and Low-cost tidal volume Monitoring and Alarming device

As introduced in chapter 1, COVID-19 has caused a worldwide health system overload and, among several consequences, a shortage of mechanical ventilators, which are critical for patient recovery in severe cases of the disease. While sharing a ventilator between multiple patients has been suggested as a last resort, the impossibility of measuring individual parameters, such as tidal volume, would create patient safety issues, risking treatment failure. This project proposes ALMA, an **A**utonomous and **L**ow-cost **T**idal volume **M**onitoring and **A**larming device to provide increased patient safety in this mechanical ventilator sharing setting.

The aim of the project was to build a low-cost, and easily-reproducible digital flowmeter, with mainly readily-available parts. These features make it helpful in times of insufficient resources and equipment, such as the COVID-19 pandemic. In an ultimate emergent shortage of ventilators, ALMA could be used to monitor tidal volume for different patients simultaneously connected to a single ventilator, when introduced to each of their inspiratory lines.

ALMA does not require any information or parameters from the ventilator and is capable of identifying the beginning and end of an inspiratory cycle by measuring flowrate. By being independent, it becomes versatile to be used alongside any brand of mechanical ventilator, and in any setting.

ALMA is a digital flowmeter, with applications in flowrate and tidal volume measurement, for mechanical ventilation settings. It dynamically analyses the gas flow in the breathing tube and displays tidal volume, integrated over the latest inspiratory cycle. Apart from performing flowrate integration, the device includes an alarm functionality that informs whether the volume detected in the line is lower

than a preset value, which can be chosen for the patient by the medical staff. The preset volume will hereafter be called target tidal volume. It is not a parameter for comparison with the ventilator, but rather a value chosen by the medical staff supervising the patient, indicating the ideal minimum volume he or she should receive over an inspiratory cycle. This will be compared to the actual volume received during each cycle.

Its interface is easy to operate, with few commands and instructions. It includes two buttons for target volume selection and alarm interruption, and an OLED display, which indicates the latest measured tidal volume and the patient's target tidal volume.

The final device consists of a measuring system, a microcontroller, buttons and a display for efficient configuration and visualization, and a visual and sonorous alarm.

This chapter focuses on the development of ALMA and the details of its operation. Section 3.1 presents an overview of the device's components and an operation diagram. Section 3.2 details the measuring system, and the steps to obtaining its response curve. It also discusses the importance of achieving adequate sensitivity for the project's goal. Section 3.3 introduces the microcontroller and programming environment, and section 3.4 explains the algorithm developed for ALMA.

3.1 Overview and Components

Project Diagram

Figure 3.1 presents the operation diagram for ALMA. Flow is admitted through a Variable Orifice Meter introduced into the patient's inspiratory line. The pressure drop generated by the air flow is then measured by a differential pressure sensor, which transmits the resulting voltage to an analog to digital converter, which in turn is connected to the microcontroller board, NodeMCU. The microcontroller is also connected to an OLED display, an LED and a buzzer, constituting the alarm, and to two buttons. These parts represent the Human Machine Interface (HMI), through which the operator will interact with the device. Power is supplied through an AC/DC adapter and a voltage regulator. Details of ALMA's development and operation will be discussed next.

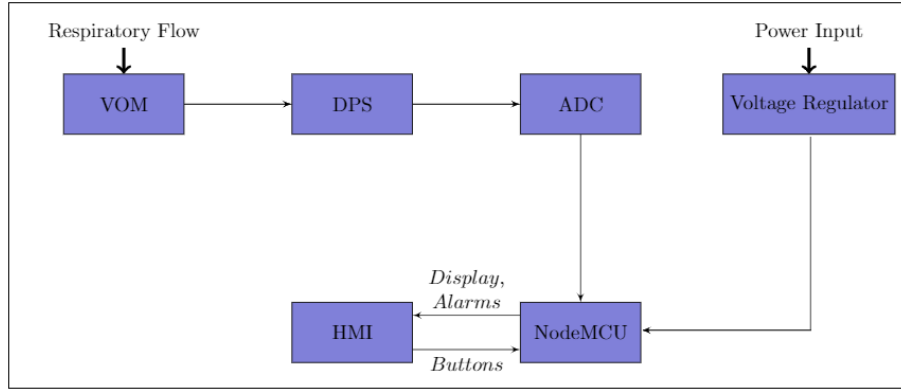


Figure 3.1: ALMA Diagram. VOM - Variable Orifice Meter; DPS - Differential Pressure sensor; ADC - Analog to Digital Converter; HMI - Human Machine Interface.

Power Source and Voltage Regulator

An AC/DC adapter, with 110/220 V input, 9 V output, 60/50 Hz, 18 W is used in this project for power supply, due to availability. Two Low Dropout Voltage Regulators (AMS1117-5.0 and AMS1117-3.3) are used to reduce switching ripple in power supply, specially for the analogical part of the circuit. The 5.0V line is used as the input for the digital part of the system (NodeMCU, buttons, display, alarm), while the 3.3V line is used as the input for the differential pressure sensor and the analog to digital converter.

3.2 Measuring System

Variable Orifice Meter and Differential Pressure Sensor

As explained in section 2.3, the measuring system consists of a Variable Orifice Meter (*VOM*), produced by Vyaire Medical, and a Differential Pressure Sensor (*DPS*), NXP model Mp3v5010dp. Flow in the *VOM* generates a pressure drop after its orifice, which is measured by the *DPS*, resulting in a voltage output. The *VOM* is the most critically available component of the device. An initial effort was made to produce an alternate orifice meter, which could be manufactured in the future. These studies will be presented in chapter 5.

Though the *DPS* presented with a known response curve between a pressure differential and its voltage output, for the *VOM*, the relationship between flowrate in the tube and resulting pressure drop was unknown. The following experiment was performed in search for the response curve of the *VOM* and the *DPS* connected i.e., a response curve between a flowrate input in the *VOM* and the voltage output in the *DPS*.

Response Curve - Flowrate versus Voltage

Testing of the measuring system was performed at the Brazilian National Institute of Metrology, Quality and Technology (INMETRO). The experiment diagram is shown in Figure 3.2. Voltage output was measured by a voltmeter, while a traceable, previously calibrated thermal mass flowmeter (model Aalborg GFM37) was placed in line with the flow, in order to provide a trustworthy flowrate reading. A fine control needle valve was used to control the air flow delivered by an air compressor. This allowed for a stable, fully developed air flow to be delivered to the circuit.

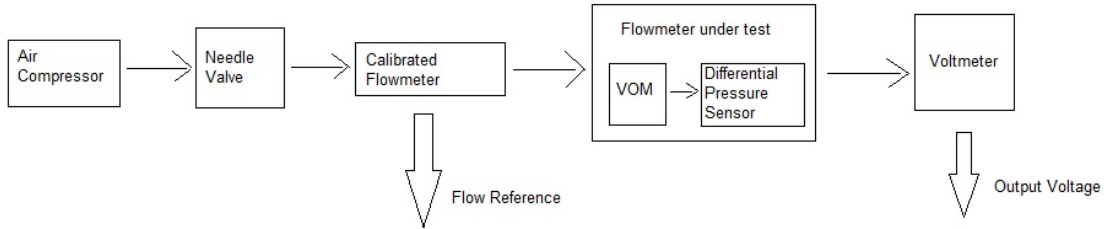


Figure 3.2: Response curve experiment

The response curve in Figure 3.3 was obtained by direct comparison between the output voltage of the meter under test and the flowrate detected by the previously calibrated flowmeter. A first order polynomial equation was generated using linear regression, resulting in Equation (3.1).

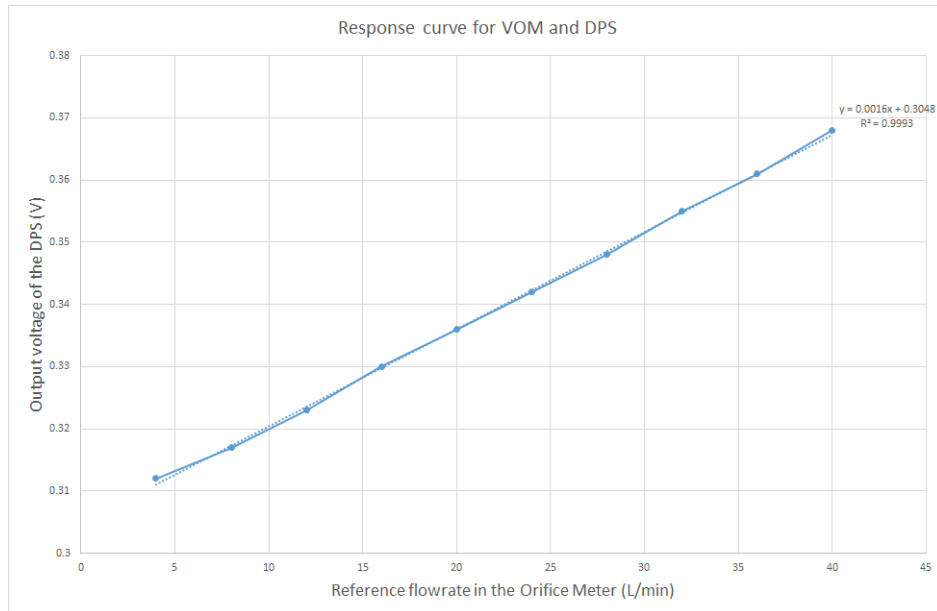


Figure 3.3: Response Curve for VOM and DPS (Output voltage versus Reference flowrate).

$$V_{out} = 0.0016 \cdot Q + 0.3048 \quad (3.1)$$

Equivalently,

$$Q = \frac{V_{out} - 0.3048}{0.0016} [\ell/min]$$

$$Q = \frac{1000}{60} \cdot \frac{V_{out}[mV] - 304.8}{1.6} [m\ell/s] \quad (3.2)$$

Where Q is flowrate, and V_{out} is the output voltage of the DPS.

Equation (3.2) will be used in the algorithm in section 3.2 to calculate instant flow, from the voltage received from the DPS. Instant flowrate will then be integrated to obtain tidal volume in the circuit.

It is crucial to consider the maximum error desired in tidal volume integration. The next two sections focus on sensitivity and the necessary precautions in analogical to digital conversion, in order to fulfill the requirement of a smaller measurement error.

Sensitivity and Analog to Digital Converter

According to *ISO80601 – 2 – 12* (Medical electrical equipment - Part 2-12: Particular requirements for basic safety and essential performance of critical care ventilators), the requirement for Inspiratory Volume Monitoring for tidal volumes greater than 50 ml, is that the accuracy of the monitoring equipment should be within $\pm(4 + (15\% \text{ of the actual inspiratory volume})) \text{ ml}$ [8]. As discussed in Chapter 1, recommendation from the Pulmonologist's Consensus on Covid-19 was to ventilate patients with 4 to 6 ml/kg [6, 7]. Therefore, for a smaller adult patient of 50 kg, receiving around 300 ml of air per cycle, it would be minimally necessary to perceive a 49 ml variation in tidal volume. Considering a standard inspiration time of 2 s, this would mean the maximum error desired for calculated instant flowrate is 24.5 $m\ell/s$.

The current measuring system presents the following sensitivity, observed in the angular coefficient in Equation (3.2):

$$\frac{\frac{1000}{60}}{1.6} = 10.4167 (m\ell/s)/mV \quad \text{or} \quad 0.096 mV/(m\ell/s)$$

It is necessary, therefore, to guarantee a discrimination threshold smaller than $0.096 \cdot 24 = 2.304 \text{ mV}$ i.e., 1 bit must represent a maximum 2.304 mV after analogical to digital conversion.

NodeMCU is equipped with an internal 10-bit Analogical to Digital Converter (ADC), which allows for one analogical input. The input voltage for the NodeMCU is 3.3 V. However, since the 10-bit resolution only allowed for a $\frac{3300mV}{2^{10}} = 3.223mV/bit$, or a $33.573 (m\ell/s)/bit$ discrimination threshold, it was considered insufficient for this project. The need to identify a $24 m\ell/s$ difference in measurement, as discussed, lead

to the choice of an external ADC with better resolution.

An Analogical to Digital converter, (Texas Instruments ADS1115 [23]) is used in order to obtain better discrimination threshold. The ADS1115 is a 16-bit, I^2C compatible converter, with a programmable amplifier gain, and 860 Hz sampling frequency. The AD converter's gain must be set in the algorithm, using the *Adafruit_ADS1015* library for Arduino IDE.

For an input between $\pm 1.024 \text{ V}$, the *ADC* provides a sensitivity of $\frac{2048 \text{ mV}}{2^{16}} = 0.03125 \text{ mV/bit}$. In ml/s , according to the calibration curve:

$$\frac{0.03125 \text{ mV/bit}}{0.096 \text{ mV/(ml/s)}} = 0.32552 \text{ (ml/s)/bit}$$

which means the system can detect a flowrate variation as small as 0.32552 ml/s .

Noise Reduction

As suggests the resulting sensitivity deduced in the previous section, 0.096 mV/(ml/s) , the measurement signal amplitude is very small for the flowrate values that will be used for ventilation, and noises as small as a few mV could cause significant reading and integration errors. Therefore, noise reduction strategies are indispensable for good accuracy.

Two measures were taken to reduce noise in signal readings. According to the suggestions on the DPS's datasheet, a capacitor was connected to its input voltage, as a decoupling filter. In addition, decoupling capacitors were connected to the ADC's input pins A0 and A1, and another was soldered between the same pins, to reject common mode noise.

Figure 3.4 shows the circuit diagram for the ADC (ADS1115), where $+5V_{CC}$ is also used as the power supply for the DPS. $C1$ is the decoupling capacitor for the DPS, placed after the 5 V voltage regulator. Capacitors $C7$ and $C8$ are decoupling capacitors for the ADC's input pins, and capacitor $C9$ is used to reject common mode noise. Capacitance values are shown in table 3.1.

Table 3.1: Capacitance Values

Component	Capacitance(μF)
$C1$	0.1
$C7$	0.022
$C8$	0.022
$C9$	0.22

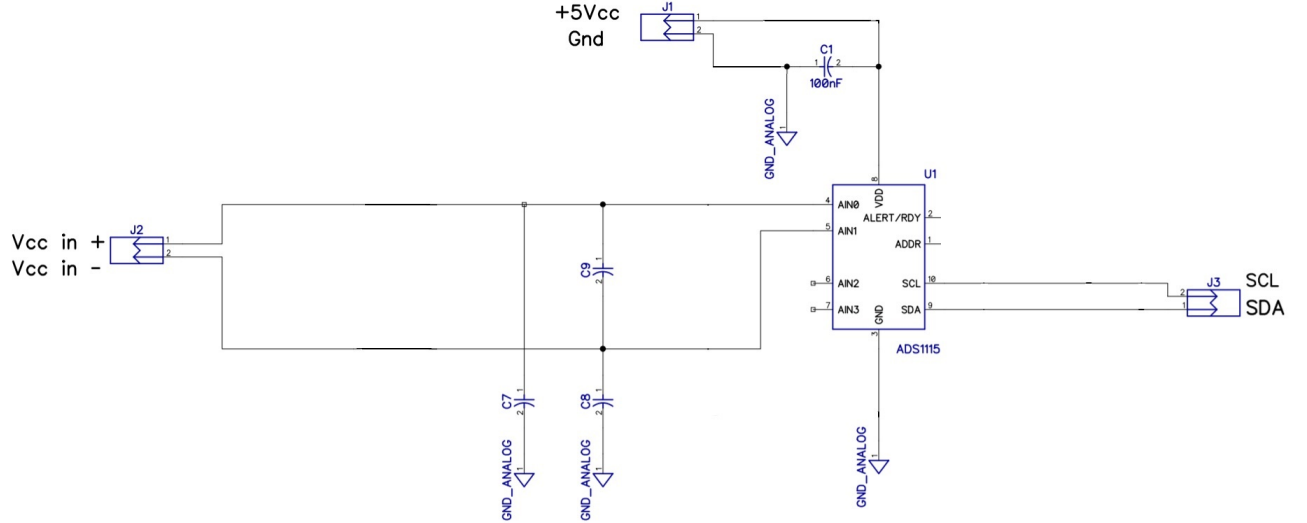


Figure 3.4: Filtering and Decoupling Circuit with ADS1115

3.3 Microcontroller Unit and Arduino IDE

NodeMcu was the chosen board for ALMA. It is an open-source firmware and development kit, based on ESP8266, which in turn is an integrated Wi-Fi MCU for IoT (Internet of Things) applications. NodeMCU was designed as an open-source, interactive, programmable, low-cost, simple, smart and Wi-Fi enabled platform. It integrates GPIO (General Purpose Input/Output), PWM (Pulse Width Modulation), IIC (a synchronous serial communication protocol), 1-Wire (a device communications bus system) and ADC (Analog to Digital Converter) pins in one board. The firmware, software which provides low-level control for the device's specific hardware, is based on Lua, but may also be programmed in C, through the Arduino IDE.

Because it integrates ESP8266 on the board with the firmware for Lua/Arduino, NodeMCU is an interesting option for prototyping IoT applications. Some of its advantages are:

- Arduino-like hardware IO (Input/Output) and coding;
- Integrated and easy to prototype;
- Low-cost;
- Wireless connection, enabled by ESP8266;
- Faster processor, compared to similar boards, such as Arduinos (NodeMCU was able to perform faster loops than an Arduino during tests for implementation, which meant a higher sampling rate, and more precise volume integration).

tion, reducing the error in discrete integration using trapezoidal method due to closer samples).



Figure 3.5: NodeMcu

Figure 3.5 is a picture of a NodeMCU, while Figure 3.6 presents its pins and their functions.

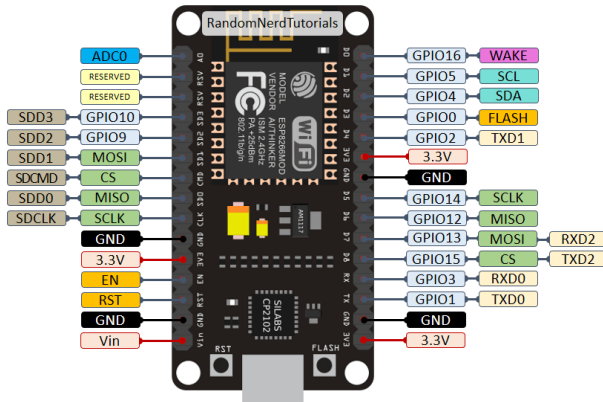


Figure 3.6: NodeMcu - pinout

The Arduino Integrated Development Environment (IDE) was used to write the algorithm and communicate with the device, and the *esp8266* package was installed to support integration with NodeMCU. The algorithm developed in the IDE is responsible for flowrate integration, alarm triggering and interface with the user, by displaying information on an OLED Display and reading input from the buttons. The *Adafruit_SSD1306* library is used to communicate with the OLED display, while the *Adafruit_ADS1015* library is necessary for the ADC.

3.4 Algorithm

As introduced in the beginning of the chapter, the goals of this project are to provide tidal volume measurement in each respiratory cycle, and to activate an alarm if the

volume is lower than a preset target value, chosen by the supervising medical team. This section presents an explanation of the algorithm developed for ALMA.

The main functionalities of the algorithm can be summarized as follows. The first step, initialization, is executed once, when the device is turned on, and before it is connected to an active flow. The main loop of the algorithm comprises the following steps: reading, processing, peak detection, integration and interface with the user. Each of them is explained next. The updated version of the code can be found on the public repository [24].

Initialization

The main purpose of this step is to initiate all variables, and to calculate the true zero of the measuring system. This value will be used in flowrate calculation, and is also set as the previous values for the first moving average calculation. Zero calibration is important to compensate for small variations on the DPS's readings. The actual value for zero pressure drop, i.e. zero flow, may vary slightly each time the sensor is turned on. It is therefore averaged over 100 samples and used during the algorithm loops.

Reading

In the beginning of each loop, the algorithm acquires information from the measurement system. Data read from the DPS by the ADC is sent to a digital input pin on NodeMCU. Current time is also read from the NodeMCU's internal clock, and stored as the reading time. This is the end of the reading phase.

Processing

A 10-point **Moving Average Filter** with rectangular window was used for noise reduction. It has shown to be very efficient to attenuate small measurement errors and random noise. The algorithm stores the 10 most recent measurements. In each iteration, the oldest value is substituted by the new measurement, and the average is calculated. The moving average filter produces a small time delay in the signal, but makes it smoother.

The moving average is then used as the input to the program's main calculations. It is first converted to mV, using the corresponding gain for the ADC's operating range. In this case, input to the ADC is ± 1.024 V, and the output is multiplied by 0.03125, its sensitivity in mV/bit. Instant *flow* is obtained by applying the response curve function to this input voltage, Equation (3.2). Finally, the *flowrate derivative* is calculated, to be used in the peak detection algorithm, developed to perceive the

beginning and end of the inspiratory cycles. Specifics of the peak detection phase will be discussed next.

Peak Detection

In order to allow ALMA to work along with any type or brand of mechanical ventilator, it was made independent of any information and parameters from the main equipment. When placed in the patient's inspiratory line, it is capable of detecting the beginning and end of the inspiratory cycle, according to instant flowrate detected in the line. The algorithm is able to decide when a new inspiration has begun, and when it ends, and defines a boolean variable which controls integration.

Figure 3.7 shows instant flowrate in blue, and its derivative in orange. As can be observed in this graph, small measurement errors during the expiratory phase (when flowrate is zero) may create a peak high enough to result in a greater derivative. This would hinder the definition of a threshold for the beginning of the inspiration phase, and could result in incorrect analysis of the flowrate curve.

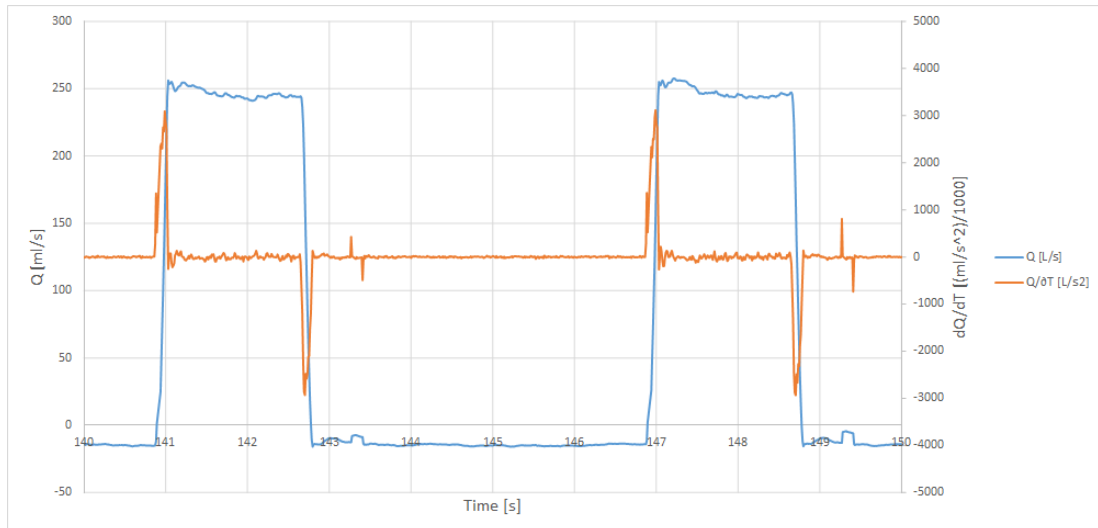


Figure 3.7: Flowrate derivative (dQ/dt) and inspiratory peak detection. The algorithm detects inspiration where the flowrate derivative surpasses a predetermined value. The flowrate (Q) is represented in blue, and its time derivative (dQ/dt), in orange.

To correct this issue, an alternate approach was used, which is shown in Figure 3.8. Instant flowrate is again presented in blue, but the grey curve now represents flowrate derivative multiplied by flowrate itself. When flowrate is smaller, this multiplication reduces errors which would cause secondary peaks in the derivative. The value is proportionally increased when flowrate is higher.

Therefore, instead of simply using the derivative of flowrate to detect the inspiratory peak, the algorithm defines a variable for $Q \cdot \frac{dQ}{dt}$, where Q is the instantaneous flowrate.

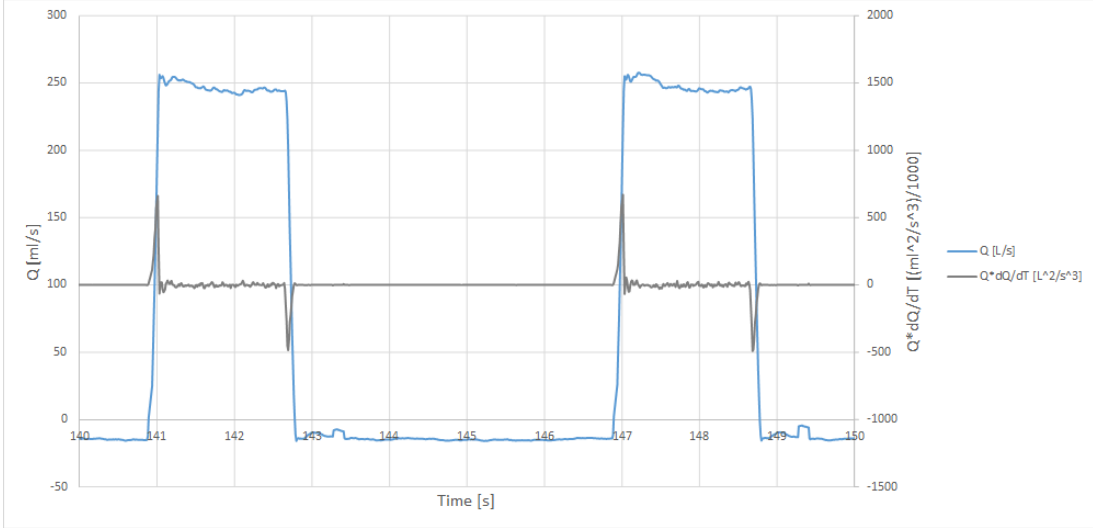


Figure 3.8: Flowrate multiplied by its derivative ($Q \cdot dQ/dt$) and inspiratory peak detection. The algorithm detects inspiration where the defined variable for $Q \cdot dQ/dt$ surpasses a predetermined value. The flowrate (Q) is represented in blue, and $Q \cdot dQ/dt$, in grey.

This option provides cleaner results when defining the beginning and end of inspiration. Notice it is easier to find a threshold for integration by evaluating the grey curve in Figure 3.8. The threshold was established by observation of the system under operational flowrate values (extreme flowrate values for mechanical ventilation). This part of the algorithm is responsible for defining integration intervals. The integration variable is made *True* during inspiration, i.e., when flowrate multiplied by its derivative surpasses the defined threshold, and *False* during expiration, i.e., when flowrate itself decreases below another set threshold.

Integration

In this step, instant flowrate is integrated over the inspiratory time, to obtain tidal volume in the latest respiratory cycle. During inspiration, flowrate is measured repeatedly. The time interval between each iteration is also the sampling time. The chosen discrete integration method was the trapezoidal method, described in the following equation:

$$V(t) = V(t_{i-1}) + \Delta t \cdot \frac{Q(t_i) + Q(t_{i-1})}{2}$$

where V is the calculated volume, Q is the measured flowrate, t_i represents time instant at the present algorithm loop, t_{i-1} , time instant in the previous loop, and $\Delta t = t_i - t_{i-1}$.

Calculated volume over the time interval is added to a storing variable, to calculate tidal volume over the whole inspiratory cycle.

Definition of the beginning and end of integration is dependent on the Peak Detection algorithm. Integration happens while the boolean integration variable is True. When the end of an inspiration cycle is detected, the integration variable is turned False, and the system **compares** the final cycle volume to the target tidal volume. The light and sound **alarm** is triggered if the volume received in a given cycle is lower than the targeted one.

Human Machine Interface/Buttons, display and alarm

The purpose of the display, buttons and alarm is to provide a simple interface for the operator. The buttons allow for target tidal volume setting, and alarm cancelling. The Adafruit 128x64 OLED Display was the choice for this project, due to availability, compactness and low cost. It was configured to present visual information of the tidal volume over the latest complete cycle, as well as the current volume target for the patient. It will also show "ALARM", from the moment the alarm is triggered, until it is cancelled by holding the alarm button. The alarm is both sonorous and visual (an LED, a buzzer and the word "ALARM" written on the screen), to facilitate identification of the patient in case of multiple alarms in a large room.

The algorithm reads information from the buttons in each loop. To avoid reading button bouncing, the code verifies the time since the last modification in status (up or down), for each button. The display is also updated in every loop.

As a configuration choice, the target selection button must be held down for 2 seconds to begin target volume selection. It should then be pressed repeatedly, cycling between the programmed volume options, which will blink on the screen. These can be easily modified in the code, but were chosen to cover expected minimum and maximum volumes for average patients, at 50 mL intervals, which should be a fair approximation for most patients. Target selection is turned off if the selection button is not pressed for longer than 3 seconds.

For the alarm cancelling button, holding it down for 2 seconds will stop all alarms. The alarm can be programmed in different ways, such as analysing multiple cycles. The purpose of the choice to trigger the alarm immediately if a cycle returns a lower value than the target was to inform the medical staff as soon as possible about any chance of poor ventilation. This gives the specialized team the decision power over patient care. Analysis over a longer timeline is enabled by the wireless and dashboard functionality, which will be discussed in the next section.

Chapter 4

Tests, Results and Discussion

4.1 Tests and Results

Testing of ALMA was performed at a hospital, by connecting the device to the inspiratory branch of a mechanical ventilator connected to a testing bag, which simulated a patient's lung. The bag's resistance and compliance were unknown, but inconsequential to the tests. The received flowrate was therefore cyclic, as it simulated breaths delivered to a patient. The following settings were defined for all tests:

- Respiratory Rate (RR): 10 cycles/min
- Inspiratory Time (T_I): 2 seconds
- Inspiratory/expiratory rate ($I : E$): 1:2
- O_2 concentration (FiO_2): 20%

Voltage output from the DPS is shown on the left, in Figure 4.1, in response to various tidal volumes, with the ventilator initially set to volume controlled ventilation. On the right, maximum voltage is compared to each tidal volume, and an approximately linear behavior is apparent.

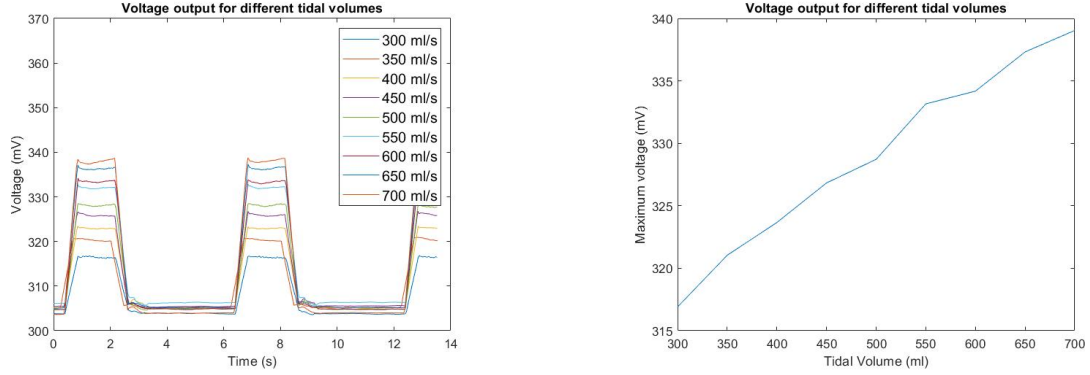


Figure 4.1: Voltage output for various tidal volumes and linear behavior

Calibration was repeated at the National Institute of Metrology, Quality and Technology (INMETRO), under constant flowrates, to provide better results. As in section 4.2, this was done by comparison to a previously calibrated flowmeter, the Aalborg GFM37 thermal mass flowmeter. Figure 4.2 shows the results obtained. Equations (4.1) and (4.2) present the response curves for voltage as a function of flowrate i.e., $V(Q)$, and its inverse.

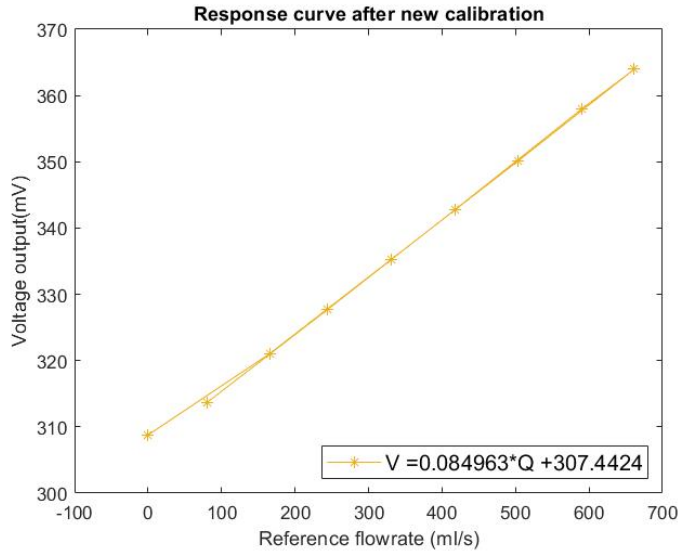


Figure 4.2: Response curve after repeated calibration

$$V(Q) = 0.084963 \cdot Q + 307.4424 \quad (4.1)$$

$$Q(V) = (V - 307.4424) / 0.084963 \quad (4.2)$$

where Q is flowrate, V is voltage, and 0.084963 is the angular coefficient to the $V(Q)$ function.

As evident in Equation (4.2), the voltage output for zero flowrate is very high, when compared to the function's first order coefficient (for a 1 ml/s variation, the voltage variation is 0.084963 mV, while 0 ml/s corresponds to 307.4424 mV). The zero value has also fluctuated over a range of approximately 5 mV between measurements.

For these reasons, in an attempt to reduce the impact of the offset instability, the voltage value at zero flowrate (v_0) is measured every time the device is switched on, and used in substitution of the linear (shift) coefficient of Equation (4.2). Equation (4.3) was used for flowrate calculations during tests.

$$Q = (V - V_0)/0.084963 \quad (4.3)$$

Tests were performed under two ventilator modes, volume control and pressure control. For volume control, the following tidal volumes were analysed: 100, 200, 300, 350, 400, 450, 500, 550, 600, 650, 700, 800 and 900 ml/cycle. For pressure control mode, the following peak inspiratory pressures were analysed: 12, 15, 18, 21, 24, 27 and 30 cmH₂O. In both modes, the first minute of measurements were discarded, while ventilation stabilized around the reference value.

Volume controlled ventilation

Results obtained under volume control mode are shown first. Tidal volume delivered and displayed by the ventilator was very stable for round volumes, multiples of 100, but varied about ± 20 ml/s for intermediate values (350, 450, 550 and 650 ml/cycle).

For each reference tidal volume, the top graph shows flowrate, in blue; and $Q \cdot dQ/dt$ (flowrate multiplied by its derivative), in orange, as shown in Figure 4.3, which presents the results for a 600 ml/cycle tidal volume.

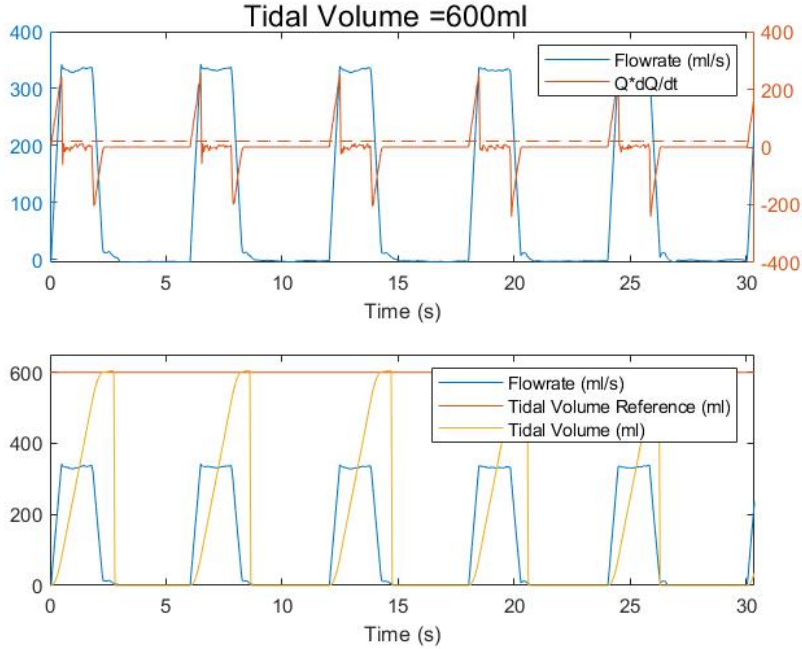


Figure 4.3: Flowrate, $Q \cdot dQ/dt$ and integration beginning threshold (top); Flowrate, programmed tidal volume, and measured tidal volume (bottom), for a 600 ml/cycle tidal volume, under volume controlled ventilation

By observing $Q \cdot dQ/dt$ for each tidal volume, a common threshold $Q \cdot dQ/dt \geq 20$ was chosen to identify the beginning of inspiration. This threshold was used to trigger the integration variable discussed in section 4.4, and is marked by the dashed orange line on the same graph. It was important to utilize a unified value for the inspiration trigger for all tidal volumes, as the device has no information on the nominal tidal volume delivered by the ventilator.

The criteria used for determining the end of an inspiratory cycle was a negative derivative and a flowrate below 5 ml/s. Although not ideally equal to zero, this threshold ensures the end of a cycle is detected in spite of small errors presented by the measuring system when flowrate equals zero.

The integration variable determines the beginning and end of volume integration. The bottom graph in each figure presents flowrate, again in blue; the nominal tidal volume programmed in the ventilator, in orange; and the volume received by the patient, in yellow, as calculated by ALMA. Volume increases during inspiration, and is reset to zero after each cycle. Figure 4.3 presents the results for 600 ml/cycle tidal volume. It is noticeable that the beginning and end of volume integration coincide with the increase and decrease of flowrate received by ALMA.

$Q \cdot dQ/dt \geq 20$ showed to be a good criteria for tidal volumes above 300 ml/cycle. The following figures present the results obtained for tidal volumes ranging from 300 to 600 ml/cycle. As previously discussed, these volumes would meet the needs of an average adult patient, weighing 50 to 100 kg, and receiving 4 to 6 ml/kg [10, 11].

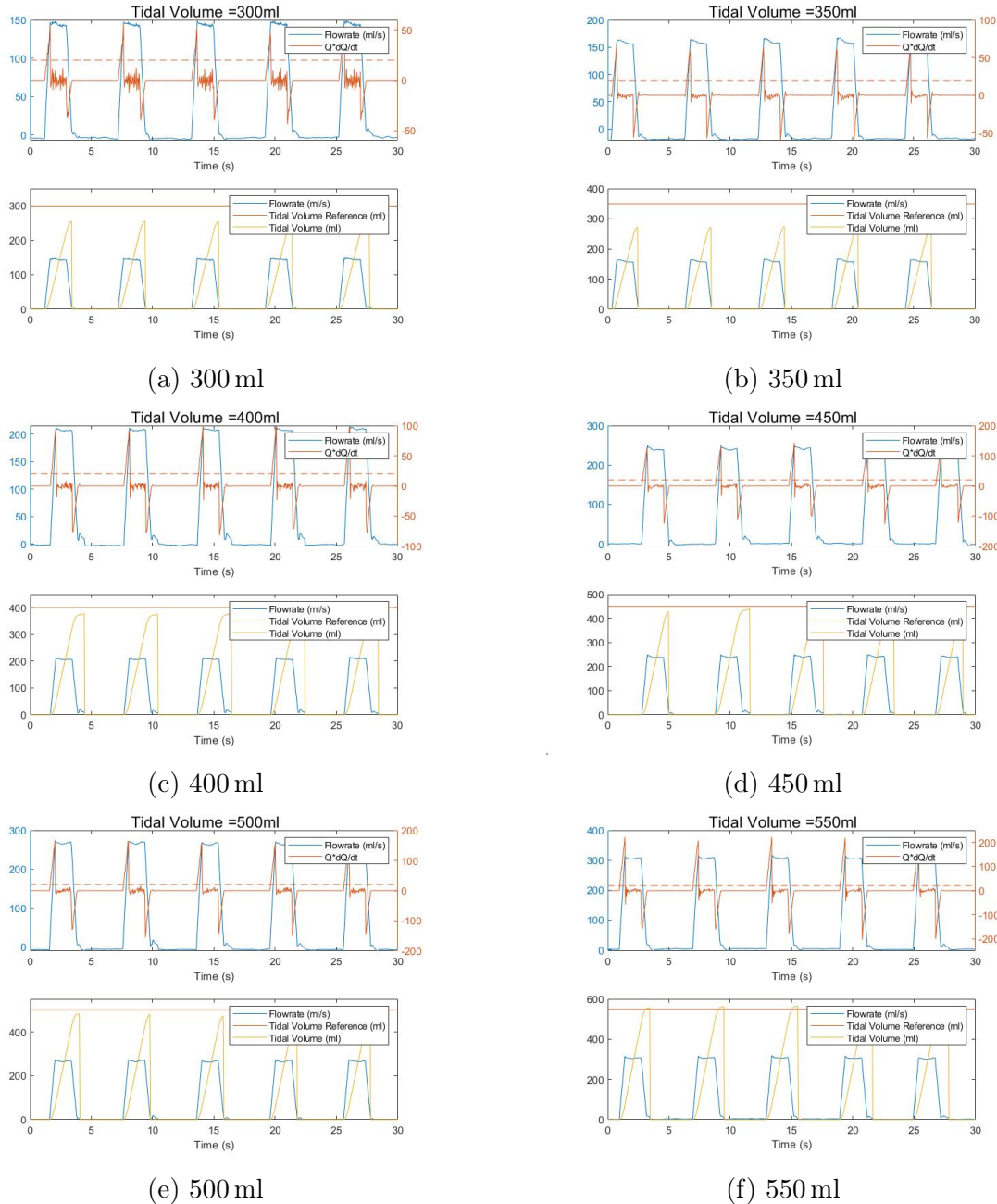


Figure 4.4: Flowrate, $Q \cdot dQ/dt$ and integration beginning threshold (top); Flowrate, programmed tidal volume, and measured tidal volume (bottom), for tidal volumes between 300 and 550 ml/cycle, under volume controlled ventilation. a) $V = 300 \text{ m}\ell$, b) $V = 350 \text{ m}\ell$, c) $V = 400 \text{ m}\ell$, d) $V = 450 \text{ m}\ell$, e) $V = 500 \text{ m}\ell$, f) $V = 550 \text{ m}\ell$.

The calculated volume was very similar to the reference volume for a 600 ml/s tidal volume, as shown in Figure 4.3, but showed errors for other tidal volumes, as can be specially noticed for a 350 ml/cycle tidal volume, in Figure 4.4. The resulting errors are presented in Figure 4.5, for all tested tidal volumes, from 100 to 900 ml/cycle. Reference volume is plotted against the maximum measured volume, for each programmed tidal volume, on the top graph. Below, error bars in measured volumes are shown, for each tested tidal volume. Results were closer to reference tidal volumes between 400 and 700 ml/cycle.

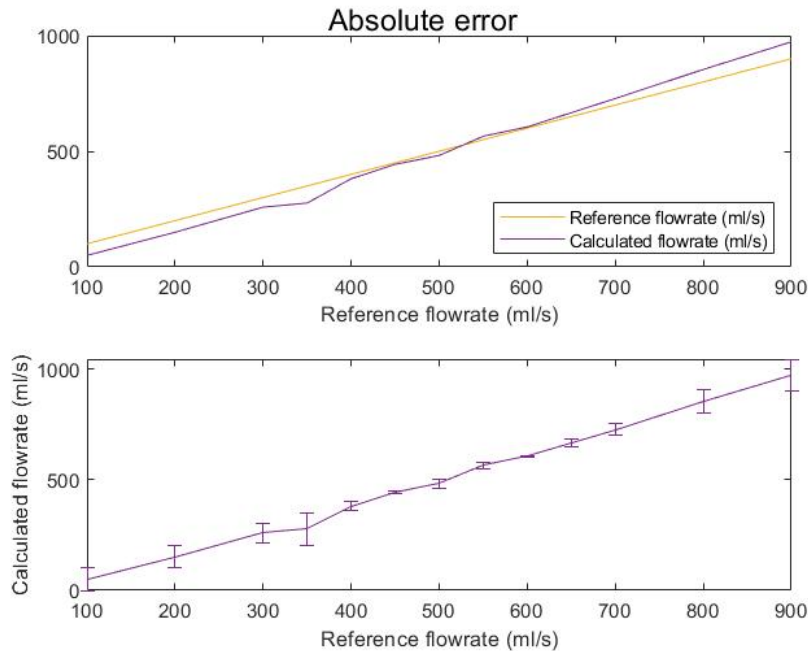


Figure 4.5: Reference volume and maximum measured volume, for each programmed tidal volume (top); Error bars in measured volumes (bottom)

ISO 80601-2-12 (Medical electrical equipment - Part 2-12: Particular requirements for basic safety and essential performance of critical care ventilators) defines the requirements for Inspiratory Volume Monitoring. For tidal volumes greater than 50 ml, the accuracy of the monitoring equipment should be within $\pm(4 + (15\% \text{ of the actual inspiratory volume})) \text{ ml}$ [8].

The results obtained under volume controlled ventilation were compared to these standards, as represented in Figure 4.6. The volume programmed in the ventilator was used as the reference volume, and is shown in black. Maximum and minimum errors for inspiratory volume, according to ISO standards, are shown in red. Finally, maximum and minimum volumes calculated by ALMA are shown in blue.

For tidal volumes between 400 and 700 ml, ALMA showed its best performance, staying well within ISO standard error limits. The error standards were also respected for 300 ml, and above 700 ml. For 100, 200 and 350 ml, the error was greater

then ISO standards. It should be noted once more that the volume delivered by the ventilator was unstable for the values of 350, 450, 550 and 650 ml. The uncertainty of the actual delivered volumes in these cases likely reflected on the increase in measurement error, which was greatest at 350 ml.

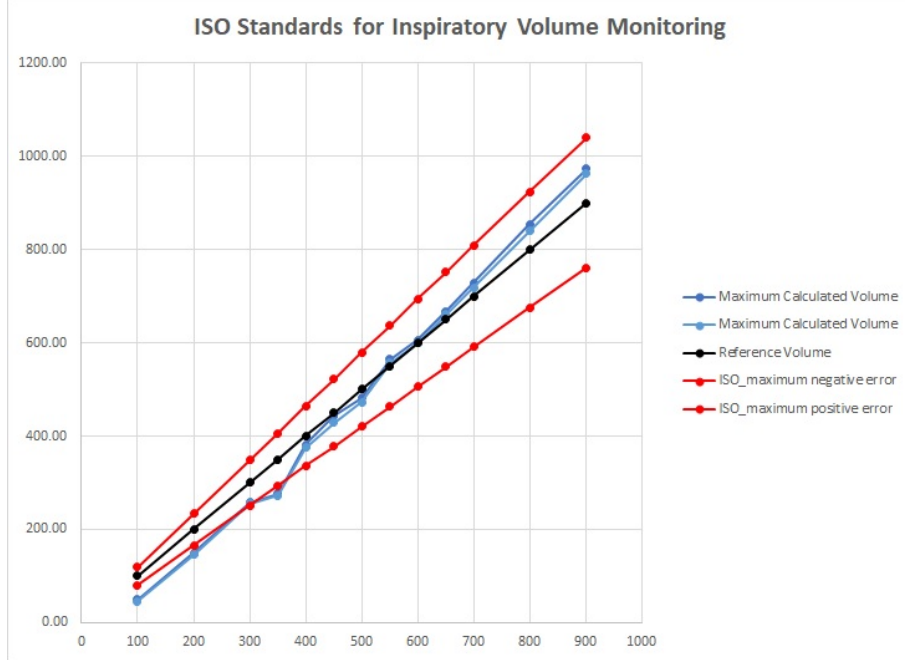


Figure 4.6: Calculated volumes compared to ISO standards for Inspiratory Volume Monitoring [8], with reference tidal volume [mℓ] programmed on the ventilator represented on the x axis.

Pressure controlled ventilation

The results obtained under pressure control mode are presented next. While volume control mode generates similarly square flowrate waves, during pressure controlled inspiration flowrate is never constant, and reaches values greater than 1500 ml/s. In this mode, the ventilator itself also measures and displays the volume delivered in each cycle. Its own internal flowmeter is also subject to uncertainties and an allowed error margin, according to ISO regulatory standards.

However reliable the ventilator's flowmeter may be, for the tests under pressure controlled ventilation there was no acquisition of the volume measured by the ventilator, since ALMA has no integration with the main ventilation device. That is so that it is independent of the ventilator's brand and model. The volume displayed by the ventilator was therefore observed and noted during the tests.

There was considerable variation in the tidal volume measured by the ventilator itself over each respiratory cycle, even after pressure stabilization in each experiment. For this reason, and also because there was no real time recording of the

reference volumes delivered, comparison between the volumes measured by ALMA and those shown in the ventilator's display was not made with the same amount of confidence as those for volume controlled ventilation, shown in the previous part of the experiments. Therefore, the following results under pressure controlled ventilation were not further evaluated to provide information on ALMA's performance, and must be further studied in future experiments.

The maximum and minimum volumes delivered were observed and noted for each pressure value set on the ventilator. These maximum and minimum reference volumes are also shown in each respective figure presented in this section, for comparison to ALMA's calculated volumes. Nominal pressure was also not always achieved by the ventilator. It was up to 1 or 2cmH₂O lower than the programmed reference, after stabilization.

Volume was calculated by ALMA according to the integration criteria defined under volume controlled ventilation. Here, $Q \cdot dQ/dt \geq 20$ was a good criteria for the integration trigger. Figure 4.7 presents the results obtained for a peak inspiratory pressure of 15 cmH₂O. The top graph displays flowrate, $Q \cdot dQ/dt$, and the threshold for beginning integration, at $Q \cdot dQ/dt \geq 20$. Below, flowrate, minimum and maximum volumes displayed by the ventilator, and volumes measured by ALMA can be observed. The same information is shown in Figure 4.8 for pressures of 12, 18, 21, 24, 27 and 30 cmH₂O.

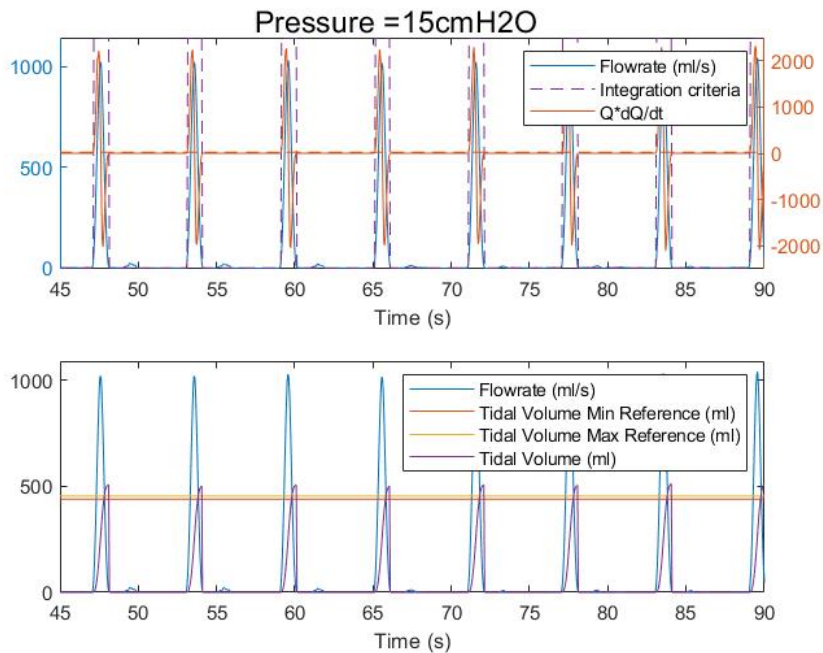


Figure 4.7: Flowrate, $Q \cdot dQ/dt$ and integration beginning threshold (top); Flowrate, minimum and maximum volumes displayed by the ventilator, and volumes measured by ALMA (bottom), for 15 cmH₂O peak inspiratory pressure, under pressure controlled ventilation

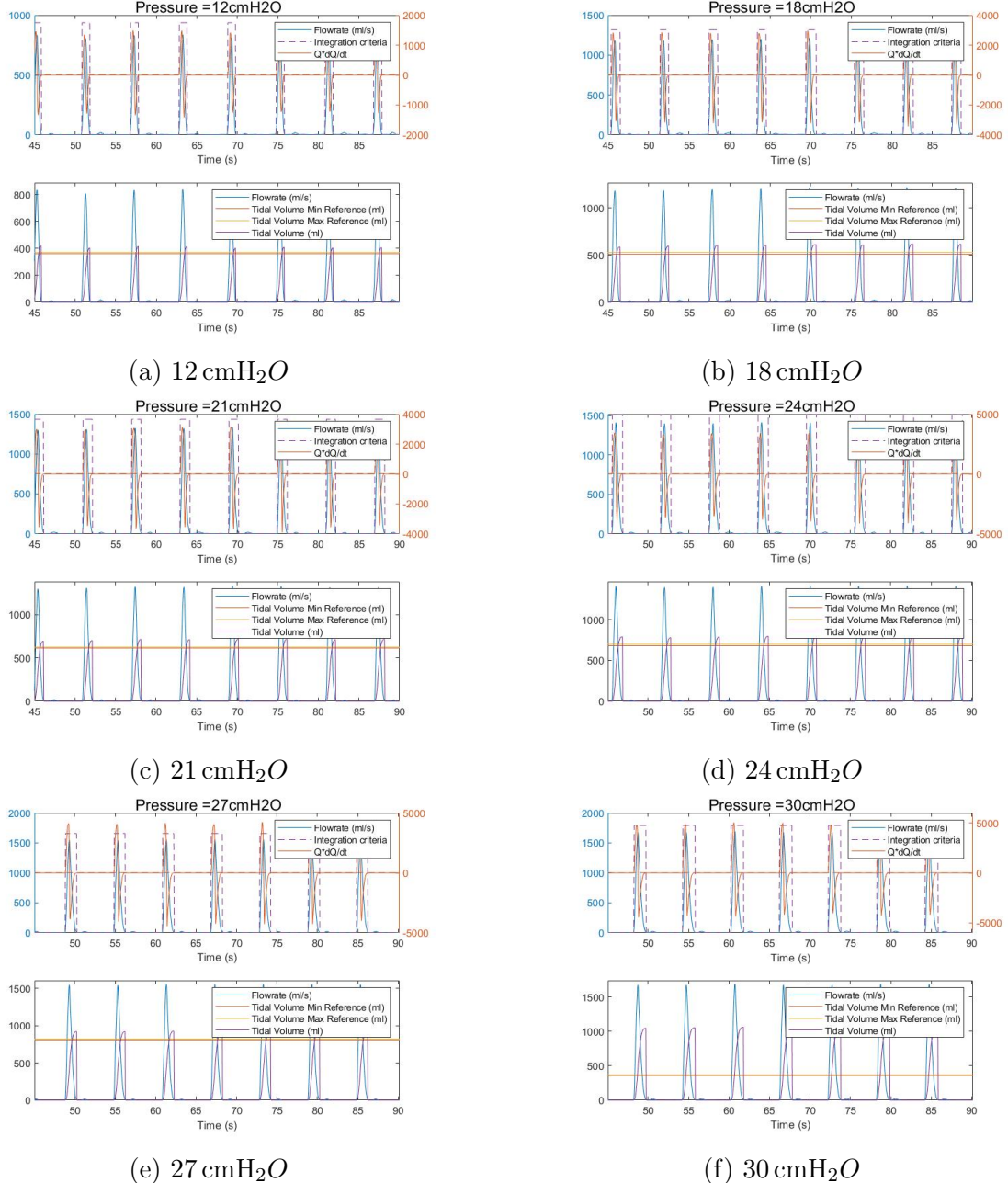


Figure 4.8: Flowrate, $Q \cdot dQ/dt$ and integration beginning threshold (top); Flowrate, minimum and maximum volumes displayed by the ventilator, and volumes measured by ALMA (bottom), for 12 to 30 cmH₂O peak inspiratory pressures, under pressure controlled ventilation. a) $P = 12\text{ cmH}_2\text{O}$, b) $P = 18\text{ cmH}_2\text{O}$, c) $P = 21\text{ cmH}_2\text{O}$, d) $P = 24\text{ cmH}_2\text{O}$, e) $P = 27\text{ cmH}_2\text{O}$, f) $P = 30\text{ cmH}_2\text{O}$.

4.2 Discussion

This work has described a low-cost and independent digital flowmeter, which may be helpful in times of insufficient resources and equipment, such as the COVID-19 pandemic. The developed flowmeter could be used to monitor tidal volume in the case of sharing a ventilator, when introduced in each patient’s inspiratory line. Other possible applications are simply as a flowmeter, to be implemented on mechanical ventilator projects or as a reliable sensor, in case of using undependable equipment.

The device does not require any information from the ventilator and is capable of identifying the beginning and end of the inspiratory cycle by measuring flowrate. It includes an alarm to inform if the patient has not achieved his target tidal volume. This target is set on the device by the supervising medical team, as an individual setting for each patient who will be using ALMA.

The focus of this project was to develop a low-cost and easily reproducible device, rather than a thorough but complex solution for ventilator sharing. The prototype was entirely developed and built in approximately 40 days, and cost under US\$ 150.00. The design is simple to reproduce and the developed software was also made available online [24]. The bottleneck of the device was the VOM, which is not easily found on the market, but can be obtained from mechanical ventilator manufacturers. This also motivated the attempt to produce an alternative piece, discussed in chapter 5.

Results presented in section 4.1 under volume controlled ventilation have shown, in comparison with ISO 80601-2-12 standards, that the prototype of the device was able of performing reasonably accurate tidal volume measurements between 400 mL and 700 mL volumes, and has shown potential for implementation in inspiratory volume monitoring applications. Future evaluation of uncertainties, repeatability, accuracy and performance under pressure controlled ventilation are necessary for further validation of the device. The DPS also shows room for improvement, as a sensor with more appropriate pressure range is recommended for a future version of the device, decreasing the need for signal filtering and enhancing. This was not the choice for the project, due to budgetary reasons, as pointed out in section 2.3.2.

For the main objective of this project, the following explanation will clarify the idea of using ALMA to increase patient safety in a shared mechanical ventilator setting. As a disclaimer, this project does not support or recommend this approach, as it presents extensive risks, as were previously discussed. However, in the context of the pandemic, this configuration of multiple patients using the same ventilator became reality in some cases. The objective is not to encourage this use, but to support the medical staff in case it is strictly necessary, by providing reliable measurements of each patient’s tidal volume.

In two existing scenarios, a ventilator may control flow based on either pressure or volume. For the event of sharing, pressure control mode would be the most adequate, since pressure recommendations are similar for patients on the same stage of the disease [10, 11]. Although a solution for increased safety in a volume-controlled system would also be possible, the complexity involved would be higher, with the inclusion of valves to control the flowrate for each patient. The speed and precision requirements for the valves and sensors in this case motivated the choice for a simplified model, limited to the pressure-controlled option. This way, the focus of this project was on lower cost and higher reproducibility with easily available parts.

The proposed solution supposes the ventilator to be on pressure control mode, in which the prescribed pressure will be maintained for all patients simultaneously by the mechanical ventilator's own control system. A group of patients should be selected, who require similar inspiratory pressure. Some implementation ideas discussed by Neyman included taking "spot compliance checks" of incoming patients, that is, each patient would be individually ventilated with an adequate fixed volume for a few cycles while recording pressure values. Patients would then only be teamed with other patients with similar lung compliance. [16].

While the ventilator should meet each of their needs, it is paramount to ensure all patients receive their optimal tidal volume. This will be done by monitoring each flow, and triggering an alarm, in case the patient does not achieve his targeted value, which will be set on ALMA by the medical team supervising the patients.

A medical team responsible for the group must evaluate each situation. If an alarm is triggered, a decision must be made whether the patient has developed different characteristics from the group (e.g. his disease has progressed more rapidly) and should be transferred to a different or even separate ventilator. Remaining limitations of the ventilator sharing setting will be discussed next.

- The system does not yet provide for the possibility of spontaneous ventilation or triggered by the patient's respiratory effort. It is exclusively a solution for mechanically controlled ventilation (ideally pharmacologically sedated and paralyzed patients).
- The respiratory parameters such as respiratory rate (RR), driving pressure ($DPress$) and O_2 inspiratory fraction (FiO_2) must be the same for all patients.
- All safety systems for possible cases of excessive pressure or leaks are dependent on the mechanical ventilator's own existing control system.
- Aiming to minimize episodes of inadequate ventilation and the need to switch patients to other ventilators, it would be more efficient to group patients with similar characteristics.

- In order to reduce differences in resistance to the inspiratory flow, circuits must have the same length and diameter. NEYMAN and IRVIN [12] suggested an arrangement of the beds in an H, centralizing the ventilator, while allowing circulation of health professionals and space optimization.
- All patients should be under the same Positive End Expiratory Pressure (PEEP). It is possible, if desired, to set up an expiratory circuit that provides different PEEP values for each patient. In this case, however, an inspiratory unidirectional valve would be needed for each patient, in order to avoid reverse flow in the inspiratory limb.
- The use of the proposed equipment is not recommended in every-day situations, due to the risk of cross-contamination. In this scenario, we assume the patients in question are all being treated for the same infection.

Chapter 5

Concluding Remarks and Future Work

5.1 Future Work

This section will present some of the work that began during the development of ALMA, and was not concluded in the scope of the project. These are possible lines of work for future development of the device. In each case, the work that has been done so far will be explained, as well as the purpose and contribution to ALMA, difficulties encountered, and possibilities as future development.

Mechanical Modelling of the VOM

Apart from being the most expensive piece in this project, the VOM was also the hardest to obtain. It is rarely in the market, since it is an important internal part of mechanical ventilators, and most producers only supply it as substitute parts, rather than separately. During the pandemic, it became as scarce as ventilators themselves. For these reasons, this project also began a study of the VOM, modeling and machining a prototype, in an effort to produce the piece at a reasonable cost.

This study was based on copying two available orifice meters. One of them was a fixed orifice meter (FOM) of pediatric size, and made of plastic. The other was a variable orifice meter (VOM), with the standard adult size and made of steel. The VOM was the piece with which ALMA was built.

The first attempt was made to machine a Fixed Orifice Meter. Figure 5.1 is a photo of a machined FOM, made at Brex Brake Systems. A few changes were made to the original model. First, the piece was made larger, in order to fit standard adult sized tubes, instead of pediatric ones. Second, because of the available drill sizes at the factory, the thickness of the opening around the orifice plate was larger than the original one. For this reason, the angle of the drilled space was recalculated,

in an attempt to better approximate the percentage of the cross section blocked by the plate. The change is visible in Figure 5.2, in which the machined parts have different angles where the orifice plate meets the external tube.



Figure 5.1: Machined FOM



Figure 5.2: Machined FOMs with smaller and larger orifice plates

The FOMs had their response curves determined through the same experiment described in section 4.2. Figure 5.3 presents the curves obtained in this experiment. The VOM, chosen for ALMA, shows significantly greater sensitivity to the flow, while also having its linearity as an advantage (curve in blue). The original pediatric FOM presented the curve in orange, while the machined FOM with the largest orifice plate generated the curve in grey. The FOM with the smaller resistance had an even smaller sensitivity, and its curve is not shown in the figure.

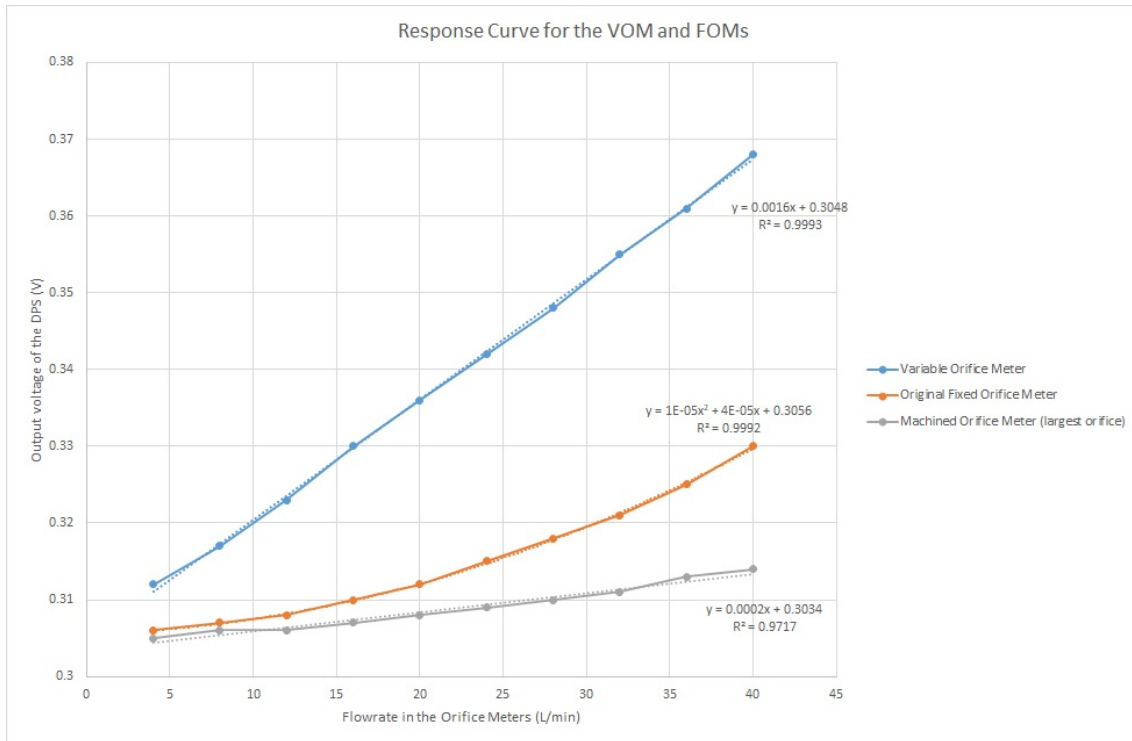


Figure 5.3: Response curves for the original VOM (blue), the original FOM (orange) and the machined FOM with larger orifice plate (grey)

After concluding the VOM would be the best option for this project, and its sensitivity would be necessary to work with the chosen DPS, the next step was to study how to produce a VOM with similar characteristics to the original one.

Figure 5.4 shows the mechanical model drawn for a VOM. It was developed in Autocad, and later Solidworks and Ansys, by measuring and copying the original VOM's parts and internal structure. By making it similar to the original one, the objective was to give it adequate mechanical characteristics, such as sensitivity, linearity, elasticity and long term resistance.

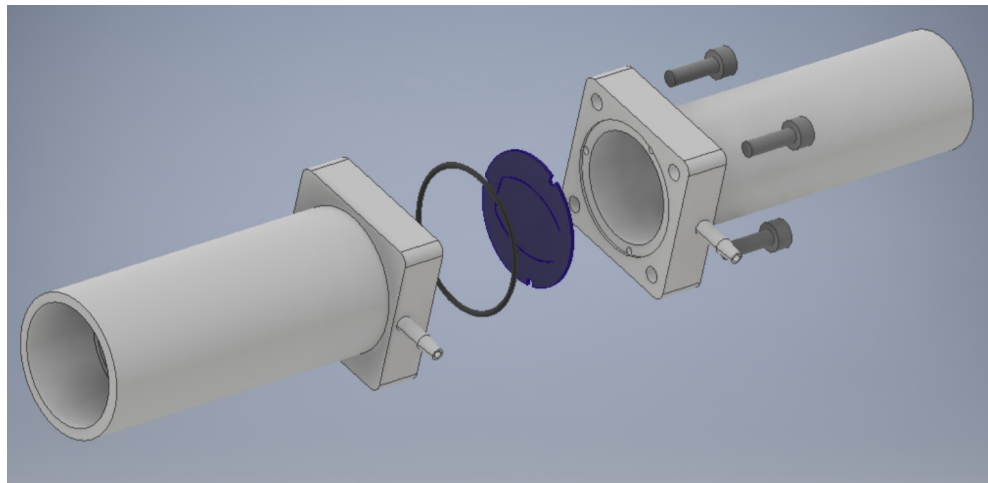


Figure 5.4: VOM mechanical model

The biggest difficulty would be to fabricate the internal resistance i.e., the orifice plate (see Figure 5.4, in dark blue). The original VOM's orifice plate was made of a 0.03 mm membrane of steel. The best possibility would be stamping the shape onto the thin plate. This option would be viable in case of a mass production of the piece, as a stamp would have to be made for the model. For this project, however, the piece was not manufactured, since only one prototype for ALMA was developed, and the original VOM was used.

Other possibilities would be to cut the orifice plate out of other materials with the right properties, so they could be allowed in medical devices, and also provide the VOM with the right pressure curve with respect to flowrate. Two materials were studied: PVC and Teflon. Their properties were used in initial stress and resistance simulations, using Ansys software. However, this scenario would need further study and development, in order to guarantee the adequate material, thickness and the shape of the cut for a useful VOM.

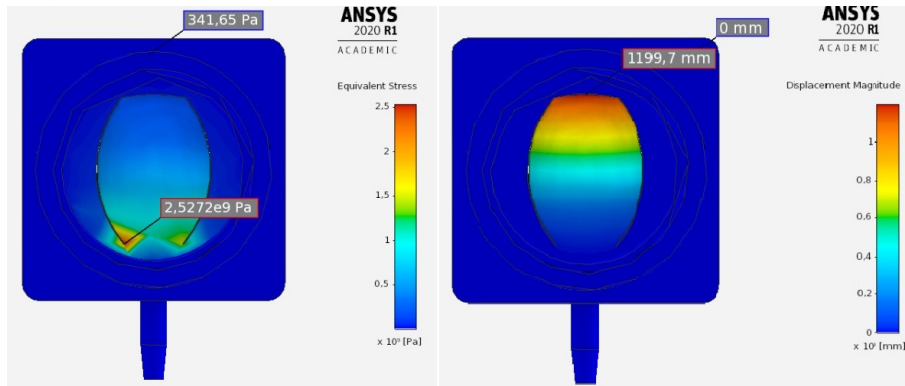


Figure 5.5: VOM model displacement and stress simulations on ANSYS software

Figure 5.5 shows some results of the simulations. To the left, material stress on the orifice plate can be visualized. To the right, displacement of the membrane can be seen. Repeated simulations and practical studies such as these would allow for elastic and plastic deformation, rupture and fatigue studies, to ensure the right material properties, and the VOM's sensitivity, linearity, stability and repeatability. As a future development, better mechanical and financial viability studies could be conducted for a real possibility of producing a VOM.

Wireless communication and data visualization

The purpose of implementing a wireless connection would be to enable analysis of patients' variables in a longer timeline. Since ALMA's display shows tidal volume in the latest complete cycle, it would be useful to provide more information by storing and displaying data elsewhere. This would also enable future use of more intelligent data analysis techniques. For instance, a group of patients connected to the same

ventilator could be monitored simultaneously to ensure their conditions remain similar over time; a larger number of patients could provide statistical representation for ventilator sharing effects in patient treatment; or a predictive algorithm could even alert the staff of a patient's deterioration earlier than the original device would have caught it by comparison.

However, the original objective would be to simply put data at the medical teams' disposal, so the analysis and interpretation of the patient's ventilatory setting and health condition would be left for the specialized staff. The programmed dashboard could receive flow, tidal volume, target volume and alarm activation information and plot them over time, making it visible over several ventilation cycles. The recipient computer would also have higher storage capacity than the microcontroller board, so it could store patient history over time.

NodeMCU is equipped with ESP8266, which would facilitate implementation. Suggested protocol for communication would be MQTT, with a few of the advantages being its small weight, low power usage, simple implementation, bandwidth efficiency, and quality of service (QoS).

Since connecting to an MQTT broker and publishing data could be sensibly time consuming in a measurement loop, specially affecting volume integration, a suggestion would be to use two NodeMCU boards. The main one would run the algorithm responsible for measurement, signal processing, peak detection, integration and interface with the user, as discussed in section 4.4. The second board would read processed information from the main one, connect to an MQTT broker and send information, by publishing the data to the patient's topic.

Data security should also be discussed in this development. Patient health information is sensitive, and must be carefully handled, specially over wireless connection. MQTT protocol also allows for security solutions, and enables message encrypting using TLS (Transport Layer Security) and client authentication with modern protocols.

Ventilator calibration project at INMETRO

Following the experiment described in section 3.2 to find ALMA's response curve, a new project began at INMETRO, with the objective of designing a testing and calibration device for mechanical ventilators and other medical equipment, with traceability to national standards. It will allow for static and dynamic calibration of gas flow to the patient (volume and flowrate), as well as pressure (absolute and differential), according to ISO 80601 standards.

ISO 80601 Part 2-12 [8] describes the particular requirements for basic safety and essential performance of critical care ventilators, beginning with the accuracy of controls and instruments. Calibration will be done in pressure-control and volume-

control ventilator modes, and inspiratory volume will also be monitored.

Figure 5.6 presents the schematics for the proposed calibration bench and portable device. The flow source for the fixed calibration bench is an air compressor. As in the experiment in section 4.2, calibration is done by comparison to a traceable and calibrated Master Meter (MM_1). The Meter Under Test (MUT) is placed inline with the MM. The future portable device will use the calibrated meter tested in the first part of the project as its master meter (MM_2).

Data acquisition is done by National Instruments's software LabVIEW, coupled with the NI 9203 and NI 9205 modules for voltage and current measurements. Temperature, pressure and gas composition will be measured in the tubes, to calculate calibration uncertainty.

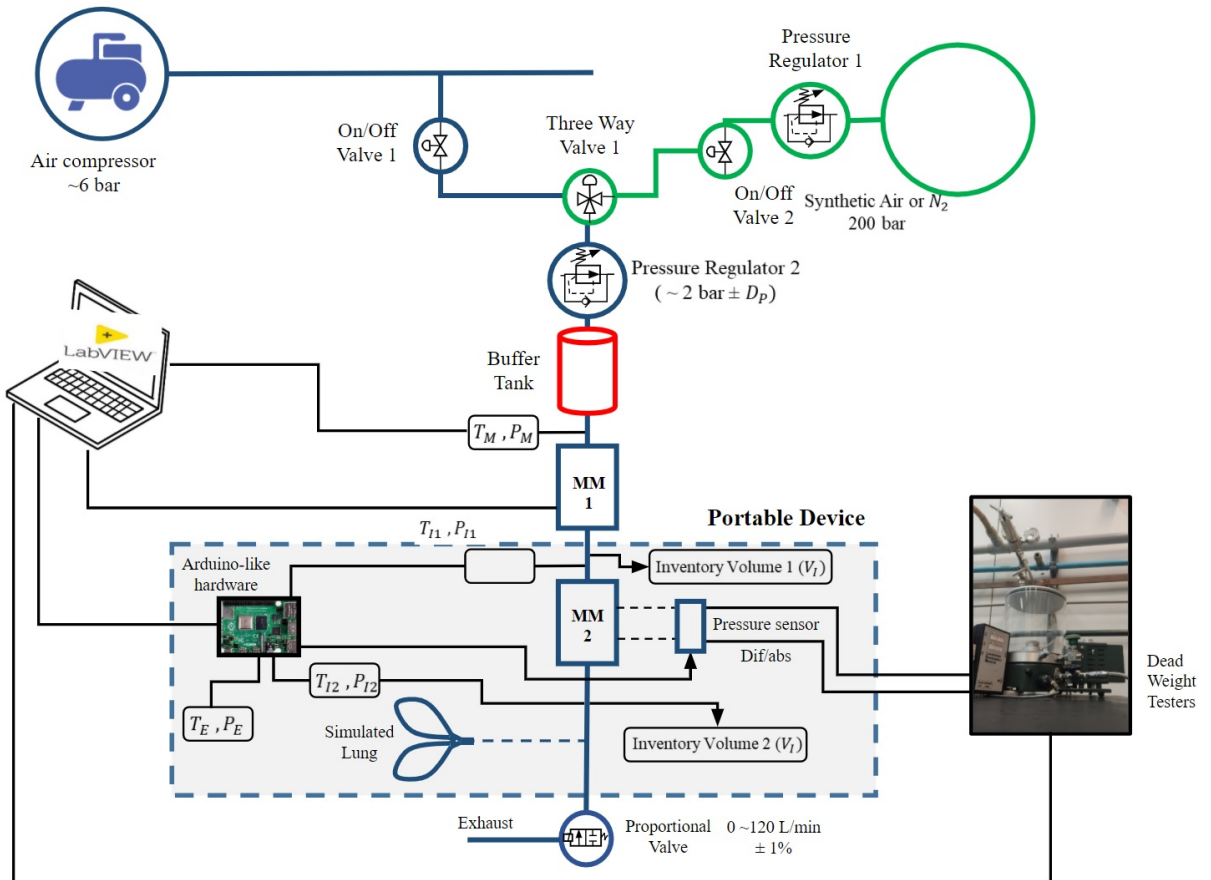


Figure 5.6: Calibration project schematics

Figure 5.7 shows the calibration bench, where the Ritter TG 05/1 drum-type gas meter performs the role of the Master Meter, while ALMA's measurement system (the VOM and the DPS) represent the Meter Under Test. ALMA's software was not used here, as the voltage output was measured by the NI module.

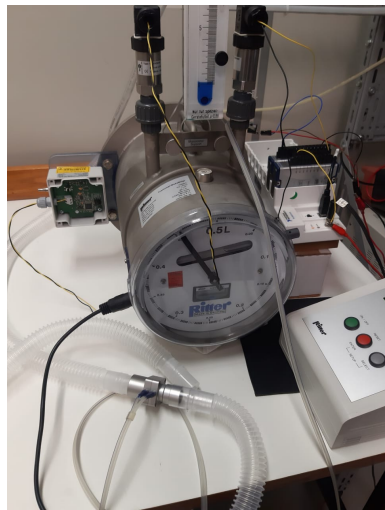


Figure 5.7: ALMA and Ritter Flowmeters

Although the drum-type meter had good accuracy, it showed large inertia, resulting in a slow response to flowrate variations. It was then substituted by the Aalborg GFM37, a thermal mass flowmeter, the same used in the experiment in section 4.2 (Figure 5.8).



Figure 5.8: Aalborg thermal mass flowmeter

The latest results are shown in Figures 5.9, where ALMA’s measurement system was used as the Meter Under Test. The voltage output of the DPS was converted to flowrate using equation (3.2) and compared to the output from the Master Meter, here represented by the Aalborg flowmeter. In Figure 5.10, the MUT’s result was processed by a 10-point moving average, in order to filter measurement noise.



Figure 5.9: Comparison between ALMA and Aalborg measurements

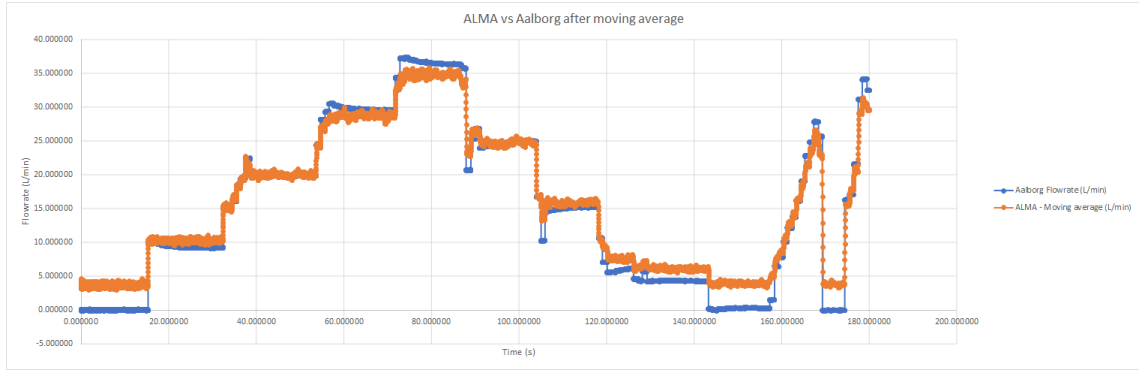


Figure 5.10: Comparison between ALMA and Aalborg measurements after Moving Average

Figure 5.11 presents recent calibration and repeatability studies for the MUT and the Aalborg flowmeter. After several calibration rounds, it is evident that the DPS (Mp3v5010dp) has an unstable zero, which is also high in comparison to the output variations under the studied flowrates. The ideal sensor should have a more suitable range and sensitivity for pressures between 0 and 200 Pa.

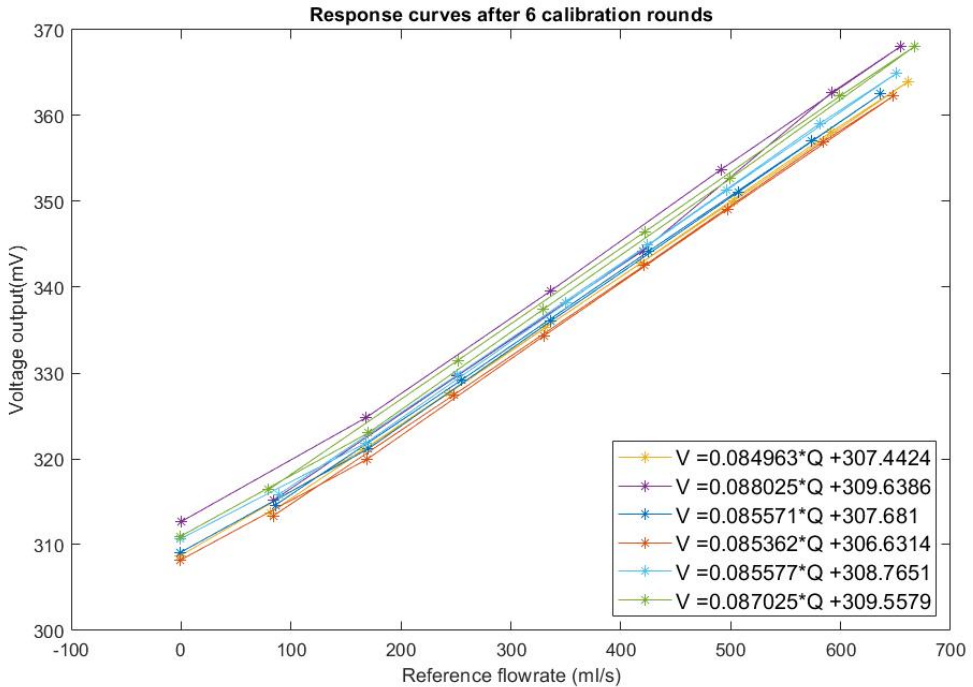


Figure 5.11: Calibration results for the MUT after 6 rounds

The Aalborg flowmeter has gas composition, pressure and temperature compensation, but presents a slower response time than ALMA’s measurement system. As disadvantages, however, ALMA’s measurement system has no in-built compensation (apart from the DPS’s) and, as discussed in chapter 4, the DPS showed small output voltage variation for the flowrates used for mechanical ventilation purposes.

Figure 5.12 shows a recent comparison between the Mp3v5010dp (ALMA’s DPS) and a more precise manometer, Furness Controls’s FCO560. Mp3v5010dp’s output voltage was converted to differential pressure, by use of its response curve, shown in figure 2.17. Mp3v5010dp’s response showed a high offset, since its sensitivity is not ideal for this range of measurements.

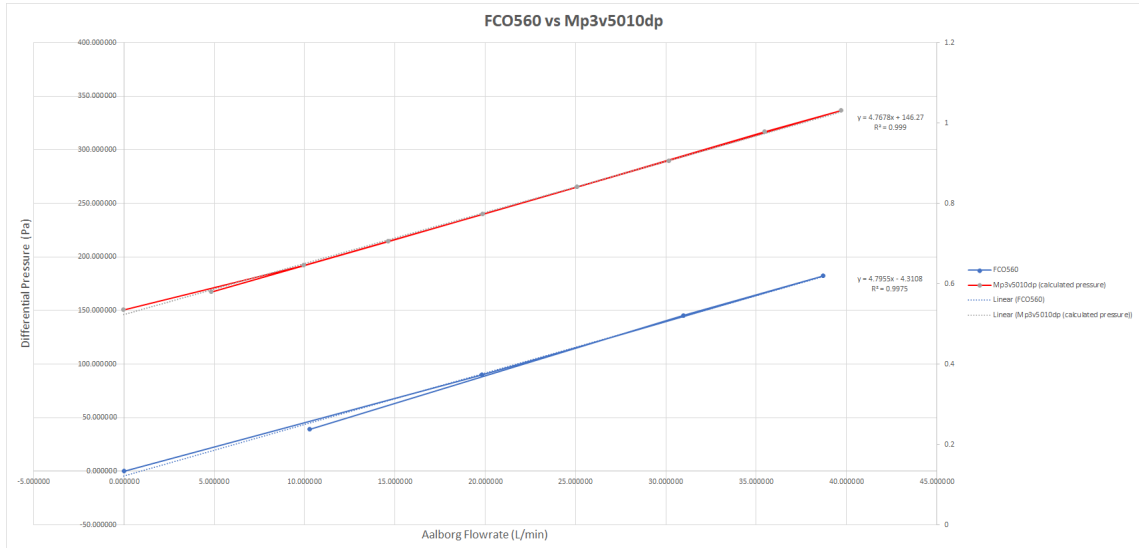


Figure 5.12: Comparison between differential pressure measurements on the VOM with the Mp3v5010dp and FCO560 sensors

The ongoing project will develop over the next few months. Flow supply is still unstable with the air compressor, and this will be dealt with by adding a pressure regulator and a buffer tank to the line. A mathematical model and the uncertainty calculations will be studied, as well as the ISO standard requirements. The portable device will be later used along with a test lung of variable resistance and compliance, in order to perform calibration of mechanical ventilation equipment.

ALMA's peak detection and volume integration functionalities will be important for cyclic measurements, when calibrating a mechanical ventilator. The software will be further developed to allow for pressure and temperature control, by actuating on pressure and temperature regulators.

5.2 Conclusion

Simulations have shown the proposed device was able to perform accurate measurement of the tidal volume delivered under volume-controlled mechanical ventilation. The error must be better studied for the pressure-controlled mode, under which the reference itself was unreliable for comparison.

The chosen differential pressure sensor, Mp3v5010dp was not ideal for the application, since its operation range was much larger than necessary for measuring the pressure drop on the VOM under mechanical ventilation. The addition of a 16-bit ADC was therefore essential to increase sensitivity, and noise reduction was also paramount for the positive outcome of the project. Moreover, the DPS's unstable zero may generate large offset problems, which were attended to in this project by measuring a zero flowrate reference each time the device is switched on.

Comparison to ISO standards showed ALMA had good performance for the expected most used tidal volumes for average patients. The initial plan was to allow monitoring between 300 and 600 ml. ALMA's performance was better between 400 and 700 ml, which is, however, a very useful tidal volume range.

The focus of this solution was to develop a low-cost and easily reproducible device, rather than a thorough but complex solution. The challenges of developing the device, from its conception to final functionality included the difficulty in obtaining parts and communicating with experienced people and organizations, as the quarantine was in place.

ALMA's uncertainty, stability and repeatability characteristics must be further studied in order to validate its reliability as a flowmeter. While the adaptation of mechanical ventilators has been debated and discouraged, a monitoring and alarming system would increase patient safety, should it happen in an absolute emergency.

Bibliography

- [1] BRIAN M. ROSENTHAL, JENNIFER PINKOWSKI, J. G. “The Other Option Is Death: New York Starts Sharing of Ventilators”. 2020. <https://www.nytimes.com/2020/03/26/health/coronavirus-ventilator-sharing.html> [Accesed: 15/03/2017].
- [2] WEST, J. B. *Respiratory Physiology: The Essentials*. Lippincott Williams and Wilkins, 2007.
- [3] 2018. <https://depositphotos.com/214608790/stock-illustration-illustration-represents-arrangement-pleural-sacs.html> [Accesed: 15/03/2017].
- [4] MELDAU, D. C. “Pleura”. 2009. <https://www.infoescola.com/sistema-respiratorio/pleura/> [Accesed: 15/03/2017].
- [5] HALL, J. E., HALL, M. E. *Guyton and Hall Textbook of Medical Physiology*. Elsevier, 2021.
- [6] TOBIN, M. J. *Principles and Practice of Mechanical Ventilation*. McGraw-Hill, 2013.
- [7] *Integrated Silicon Pressure Sensor On-Chip Signal Conditioned, Temperature Compensated and Calibrated*. NXP, 2009. Rev 0, 4.
- [8] ISO 80601-2-12. *Medical electrical equipment - Part 2-12: Particular requirements for basic safety and essential performance of critical care ventilators*. Relatório técnico, International Organization for Standardization, 2020.
- [9] <https://www.who.int/emergencies/diseases/novel-coronavirus-2019/question-and-answers-hub/q-a-detail/q-a-coronaviruses> [Accesed: 06/19/2020].
- [10] “International Pulmonologistâs Consensus on Covid-19”, 2020.
- [11] “International Pulmonologistâs Consensus on Covid-19 2nd Edition”, 2020.

- [12] NEYMAN, G., IRVIN, C. B. “A Single Ventilator for Multiple Simulated Patients to Meet Disaster Surge”, *Society for Academic Emergency Medicine*, 2006.
- [13] PALADINO, L., SILVERBERG, M., CHARCAFLIEH, J. G., et al. “Increasing ventilator surge capacity in disasters: ventilation of four adultâhumanâ-sized sheep on a single ventilator with a modified circuit”, *Resuscitation*, 2008.
- [14] BRANSON, R. D., BLAKEMAN, T. C., ROBINSON, B. R., et al. “Use of a single ventilator to support 4 patients: laboratory evaluation of a limited concept”, *Respir Care*, 2012.
- [15] HESS, D. R., KACMAREK, R. M. *Essentials of Mechanical Ventilation*. McGraw-Hill, 2019.
- [16] BRANSON, R., RUBINSON, L. “A single ventilator for multiple simulated patients to meet disaster surge”, *Society for Academic Emergency Medicine*, 2006.
- [17] BRANSON, R., RUBINSON, L. “One ventilator multiple patients - What the data really supports”, *Resuscitation*, 2008.
- [18] CAVANILLES, J. M., GARRIGOSA, F., PRIETO, C., et al. “A Selective Ventilation Distribution Circuit (S. V. D. C.)”, *Intensive Care Medicine*, 1979.
- [19] SOLIS-LEMUS, J. A., COSTAR, E., DOORLY, D. J., et al. “A Simulated Single Ventilator / Dual Patient Ventilation Strategy for Acute Respiratory Distress Syndrome During the COVID-19 Pandemic”, 2020.
- [20] RAREDON, M. S. B., FISHER, C., HEERDT, P., et al. “Pressure-Regulated Ventilator Splitting (PReVentS): A COVID-19 Response Paradigm from Yale University”, 2020.
- [21] “Joint Statement on Multiple Patients Per Ventilator”, *Anesthesia Patient Safety Foundation (APSF)*, 2020.
- [22] SCHENAA, E., MASSARONI, C., SACCOMANDI, P., et al. “Flow measurement in mechanical ventilation: A review”, *Medical Engineering and Physics*, 2015.
- [23] *ADS111x Ultra-Small, Low-Power, I 2C-Compatible, 860-SPS, 16-Bit ADCs With Internal Reference, Oscillator, and Programmable Comparator*. Texas Instruments, 2018.

- [24] PIMENTA, M. T. “Increasing Safety in Mechanical Ventilator Sharing”. <https://github.com/marianatpimenta/IncreasingSafetyInMechanicalVentilatorSharing>, 2020.